Journal of the Geological Survey of Brazil

The role of intracratonic crustal reworking in the tectonic compartmentalization of the Juruena Terrane, SW Amazonas Craton: the Roosevelt-Guariba Transpressive Belt

Antonio Charles da Silva Oliveira[1,3*], Marcelo Esteves Almeida[2,3]

[1]Serviço Geológico do Brasil – SGB/CPRM. Av. André Araújo 2010, Manaus, Amazonas, Brazil, CEP:69.067-375
[2]Serviço Geológico do Brasil – SGB/CPRM. Departamento de Recursos Minerais. Avenida Pasteur, 404, Urca, Rio de Janeiro - RJ, Brazil, CEP: 22290-255
[3]Programa de Pós-Graduação em Geociências – PPGGEO. Universidade Federal do Amazonas – UFAM. Campus Universitário Sen. Arthur Virgílio Filho (setor norte), Av. Gen. Rodrigo Octávio Jordão Ramos, 6.200, Manaus, Amazonas, Brazil, CEP:69.080-900

Abstract

The multiscale structural analysis carried out in the NNW sector of the Juruena Terrane, SE of the State of Amazonas combines structural mapping, microtectonic analysis and aeromagnetic data analysis. The terrane shows a complex structural and metamorphic history composed of successive deformation events, responsible by the formation of its tectonic framework. Event D2 (1520-1460 Ma) is responsible for the main structure of the NNW sector of the Juruena Terrane, and it generates a dextral transpressive NW-SE-trending shear zone, called Roosevelt-Guariba Transpressive Belt (RGTB). This is an intracontinental high-temperature, medium-pressure tectono-thermal event, compatible with the conditions of the upper amphibolite to granulite facies. The RGTB controls the tectonic compartmentation of the region, particularly affecting the Granitic Gneiss Domain (1760-1750 Ma). Other sectors, such as the Supracrustal Rock Domain (1800-1730 Ma) and the Pre-Juruena geological-structural association (>1830 Ma), are subordinately affected. Event D2 overlaps the regional structure E-W (ENE-WSW) attributed to D1 (1690-1630 Ma), which is restricted to the deep basement in the NNW sector, but dominant in the south central sector of the Juruena Terrane. There are also two late brittle-ductile to brittle deformation events (D3 and D4). Event D3 (1320-1300 Ma) is represented by NE-SW cataclastic and shear zones, commonly serving as conduits for hydrothermal fluids relative to gold mineralization. Event D4 is comprised of normal faults and fractures that reactivate RGTB shear zones, limiting Neoproterozoic and Paleozoic-Mesozoic sedimentary exposures. The tectonic structural model proposed in this study reinforces the interpretation that the Juruena Terrane evolved from a foreland basin, which was formed during the Juruena Orogen and whose basement is the Orosirian Tapajós Crust. This basin was preserved from the tectono-thermal effects of the end of the Statherian (D1), and it was only during event D2, after emplacement of the RGTB, that it underwent high-grade deformation and metamorphism, whose driving force is attributed to the stress propagation in pericratonic regions, associated with Calymmian orogens. The successive events are related to the cratonization of the Juruena Terrane, represented by late crust reactivation (D3) and neotectonic events (D4).

Article Information

Publication type: Research papers
Received 25 May 2021
Accepted 13 July 2021
Online pub. 26 August 2021
Editor: Vladimir Medeiros

Keywords:
Lithospheric shear zone
Intracontinental deformation
Structural geophysics
Multiscale
Juruena Terrane
Amazon Craton

*Corresponding author
Antonio Charles da Silva Oliveira
charles.oliveira@cprm.gov.br

1. Introduction

Shear zones record relative motions of crustal blocks. The structural style and the overprinting relationships in these zones provide key information about displacement and kinematics, which can define the relative chronology of transport and tectonic deformation, in addition to providing information about crustal reactivations and reworking (Holdsworth et al. 2001). Lithospheric shear zones control the geotectonic framework of many Proterozoic terranes, and the longevity of these megastructures results in successive superimposed deformational fabrics, in which each new event partially obliterates or destroys previous fabrics, generating complex structural geological histories.

In stable continents, basements are commonly restricted to small and isolated exposures; therefore, it is difficult to determine the relationships between detailed geological-structural observations and regional tectonic evolution. This is particularly the case for the NNW sector of the Juruena Terrane, SW of the Amazon Craton. It is a region with difficult

ISSN: 2595-1939
https://doi.org/10.29396/jgsb.2021.v4.n2.3
Open access at jgsb.cprm.gov.br

access, vast tropical forest cover, recent sedimentary covers and a thick weathering mantle.

The Juruena Terrane, together with the Jamari and the Jauru terrains, form the Rondônia-Juruena Province (Santos et al. 2000) or the Rondoniano-San Inácio Province (Tassinari and Macambira 1999). This land is an E-W trending belt, inflecting to NW-SE, with approximately 1100 km long and 350 km wide (Scandolara et al. 2017), contrasting with the NW-SE regional structure attributed by the mobilist models for the Amazon Craton (Santos et al. 2008; Cordani and Teixeira 2007).

In the SE of the State of Amazonas, the Juruena Terrane has a major NW-SE structure represented by a system of shear zones and faults, known as the Roosevelt-Guariba Transpressive Belt (RGTB, in this paper). Although the geodynamic models proposed for the region are tectonically antagonistic, these models consider the evolution of RGTB as part of the architecture of the Juruena terrane. Rizzotto et al. (2019b) showed that high-grade rocks (Nova Monte Verde Complex) are affected by the RGTB, assuming a taphrogenic model (Tapajós rift) in which a Metamorphic Core Complex developed between 1800-1763 Ma (Rizzotto et al. 2019a). Scandolara et al. (2017) interpreted this structure as the result of a DE1 event, with a metamorphic peak between 1.69-1.63 Ga, and these NW-SE shear zones represent frontal and oblique ramps with vergence from SSW to NNE, associated with the Juruena Orogen.

In this paper, we demonstrated and confirmed the relationship between geological structures and potential geophysical data through structural geophysical analysis (Jessell et al. 1993; Jessell and Valenta 1996; Betts et al. 2003, 2007; Steward and Betts 2010; Direen et al. 2005). Aeromagnetometric data provided continuity between observations of outcrop discontinuities to enable the redesign of the crustal architecture in the NNW portion of the Juruena Terrane. This approach integrates data from multiple sources at different scales, aiming to describe the structural and metamorphic history of the RGTB and its implication for the evolution of the Rondônia-Juruena Province, Amazon Craton.

2. The Juruena terrane in the southwestern Amazon Craton

Located in the SE region of the State of Amazonas, the study area is inserted in the NNW portion of the Juruena Terrane, Roosevelt-Aripuanã Domain (Reis et al. 2006), a part of the Rio Negro-Juruena Province (1.80-1.55 Ga; Cordani and Teixeira 2007) or the Rondônia-Juruena Province (1.82-1.54 Ga; Santos et al. 2008), and composes the SW portion of the Amazon Craton.

The Rondônia-Juruena Province (Figure 1A) has an elongated shape NW-SE, delimited by the Tapajós-Parima and Sunsás provinces, to the northeast and southwest, respectively. To the north and south, it borders the sedimentary covers of the Parecis and Amazon basins. It evolved from geological accretion of magmatic arcs and soft collision, between 1.82 and 1.54 Ga, generating a terrane with contributions from juvenile sources and older material (Tapajós Crust), as shown by εNd(T) data, with values ranging between +3 and -3, and T_{DM} model ages between 2.1 and 1.9 Ga (Assis 2011; Cordani et al. 2009; Lacerda Filho et al. 2004; Leite et al. 2001; Santos 2003; Scandolara et al. 1995).

Scandolara et al. (2017) reaffirmed the accretionary origin of the Juruena Terrane for the region by proposing an orogenic model (Figure 1B), consisting of the Jamari and Juruena magmatic arcs, generated in an Andean-type active continental margin setting (Duarte et al. 2012; Ribeiro and Duarte 2010; Rizzotto and Quadros 2005; Santos 2003; Santos et al. 2000; Scandolara et al. 2014, 2013; Souza et al.

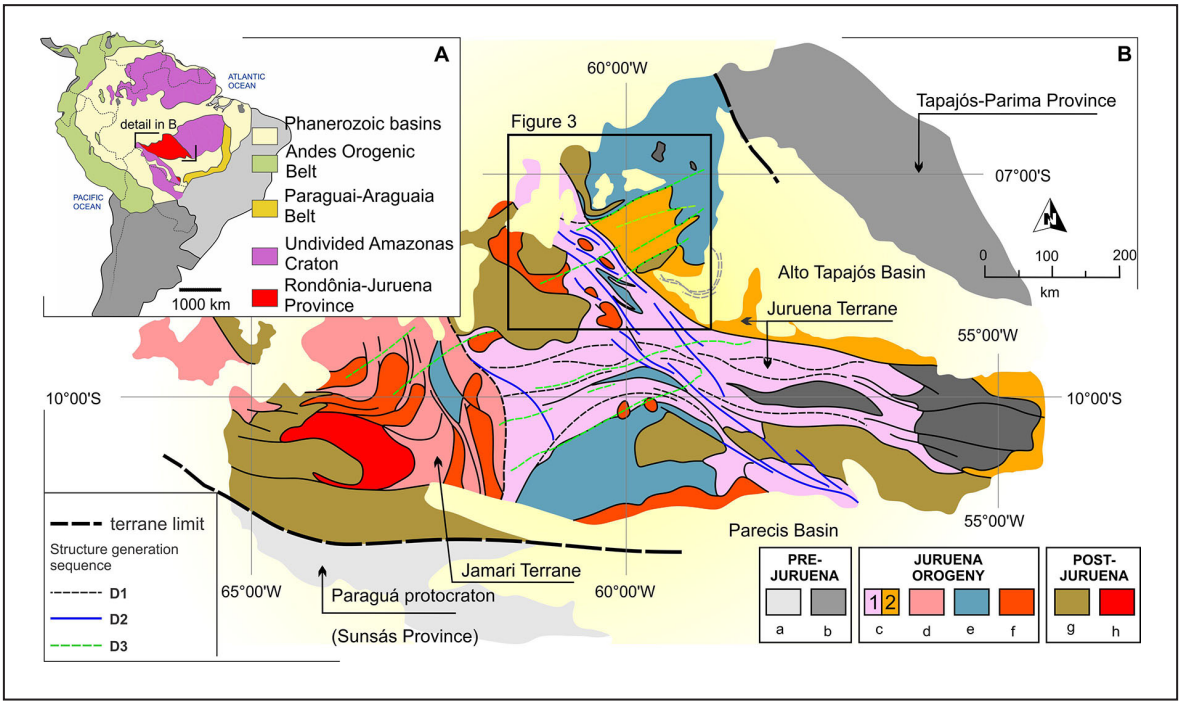

FIGURE 1. A) Map of the South American Platform highlighting the Rondônia-Juruena Province in the Amazon Craton (Santos et al. 2008); B) simplified geotectonic map of the Juruena Terrane (according to Scandolara et al. 2017). Caption: Tapajós-Parima Province (a) and Paraguá Protocraton (b); Juruena (c) and Jamari (d) complexes, orogenic basins (e), post-orogenic magmatism (f), intracratonic basins (g) and anorogenic magmatism (h).

2005; Tassinari and Macambira 1999). However, Montavão et al. (1984) and Neder et al. (2000) consider the Jamari and Juruena Terranes as having been generated in an intraplate extensional setting related to the late- to-post-tectonic phases of the Tapajós-Parima Orogeny (2.00-1.88 Ga; Pinho et al. 2003). Recently, Rizzotto et al. (2019a, 2019b) redefined the Juruena Terrane as the Western Amazon Igneous Belt. An evolution in an intraplate extensional tectonic environment (Tapajós-Parima Rift) is admitted in response to underplating of mafic magma at the base of the crust. There are also alternative proposals, which admit a model of hot orogens (Collins 2002) to describe an evolution with alternation between extensional and compressional events in a plate margin environment, in response to variations in slab subduction angle (Alves et al. 2013; Diener et al. 2019; Duarte et al. 2019; Trindade Netto et al. 2020).

3. Materials and methods

In addition to field data collection, this study used geological data from geological mapping projects and metallogenic studies carried out by the Geological Survey of Brazil, available on the GEOSGB portal (www.geosgb.cprm.gov.br). Geophysical data were extracted from airborne surveys in Aripuanã (CPRM 2010a), Sucunduri (CPRM 2010b) and Rio Branco-Machadinho (CPRM 2015), also available on the GEOSGB portal. These magnetometric and gamma spectrometric aerial surveys have north-south flight lines 100 m high and spaced 500 m apart.

The collected data were integrated and then underwent multiscale structural analysis, following the precepts of structural geophysics (Jessell et al. 1993), a method that, based on the fractal concept of invariability as a function of scale (Hippertt 1999; Turcotte 1997), applies structural analysis techniques to geophysical data (Betts et al. 2019 and references therein).

Particularly to delineate the structural framework in the NNW portion of the Juruena Terrane, aeromagnetic data processing routines were applied to enhance the magnetic responses of structural features at different depths. The Gaussian filter was applied to the magnetic anomaly data (Figure 2A) (Jacobsen 1987; Oliveira 2008). The parameters used in this filter were defined by analyzing the average radial power spectrum (Spector and Grant 1970, Figure 2B),

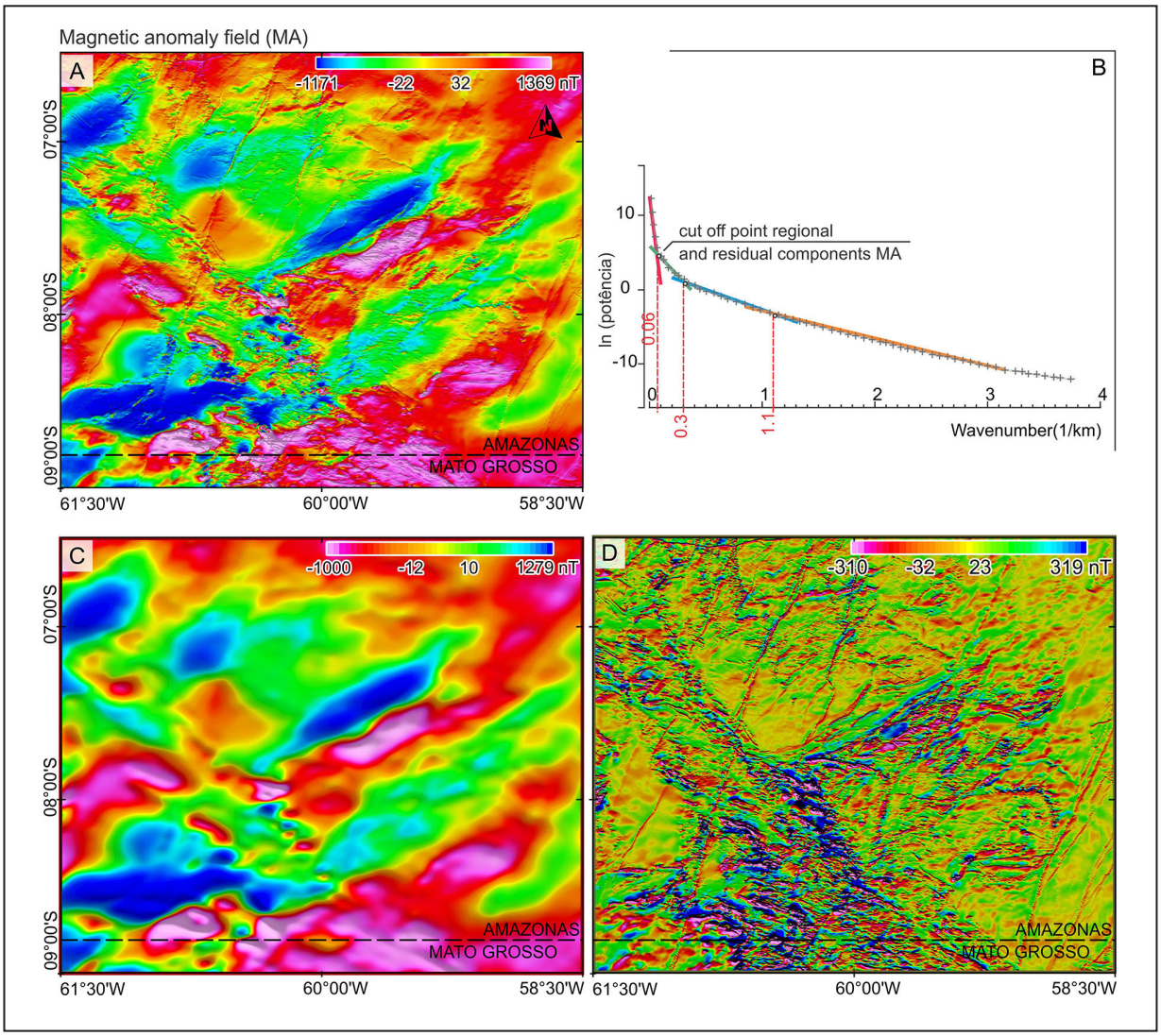

FIGURE 2. A) Magnetic anomaly (MA) map of the NNW portion of the Juruena Terrane. B) Average radial power spectrum graph. C) and D) Estimation of magnetic anomaly depth, highlighting the wavenumber (0.06) used in the Gaussian separation filter for regional (>16 km) and residual (<16 km) sources, respectively.

generating magnetic anomaly images of regional components (Figure 4A), magnetic sources with depths greater than 16 km, residual magnetic anomaly (Figure 4C), and sources with depths between 16 km and 900 m.

The structural interpretation of the geophysical images was based on the premises established by Betts et al. (2007), Leseane et al. (2020) and Stewart et al. (2009). These are the major ones: magnetic anomalies are the product of lithological contrasts within the shallow crust; therefore, magnetic lineaments are the product of deformation in horizontal axes, such as shortening, tilting, bending or faulting of a stratigraphic package with internal magnetic contrasts; truncations or deflections of magnetic anomalies indicate the location of shear zones, faults or fractures; and rotation or displacement of anomalies indicate apparent motion.

4. Tectonic compartmentation of the NNW of the Juruena Terrain

In the last decade, as a result of geological mappings, geophysical aerial surveys and metallogenic studies, geological and stratigraphic features of the NNW of the Juruena Terrane could be studied in more detail and then updated (Albuquerque et al. 2017; Almeida et al. 2016; Brito et al. 2010; Goulart and Silva 2019; Oliveira and Lira 2019; Reis et al. 2013; Reis and Ramos 2017; Simões et al. 2020- Figure 3). For the present study, the mapped units were grouped into geological-structural associations (Pre-Juruena, Juruena, Post-Juruena).

The pre-Juruena geological-structural association includes Orosirian units represented by metasedimentary sequences of the Abacaxis Formation (Santos et al. 2000), and A-type granitic intrusions, represented by the Chuim (1855 Ma) and Arraia (1838 Ma) porphyritic granites (U-Pb LA-ICP-MS in zircon, Meloni et al. 2018). Meloni et al. (2018) attributed these units to the basement of the region, considered as a continuity of the Tapajós-Parima Province.

The Juruena geological-structural association brings together the late-Orosirian and Statherian units of the Juruena Terrane, subdivided into domains of supracrustal rocks (SCD) and granitic gneiss (GGD). In SCD, the supracrustal rocks do not show deformation and metamorphism, and they are represented by the Colíder Group (Frasca et al. 2002), composed of felsic volcanic rocks, with rare intermediate and mafic members, aged between 1820 and 1787 Ma (U-Pb SHRIMP and LA-ICP-MS in zircon; Almeida et al. 2016; Pinho et al. 2003); and of the Vila do Carmo Group (1744-1570 Ma, Reis et al. 2013). The latter represents a volcanic-sedimentary rift basin associated with taphrogenic tectonic events, which were widespread around the world and preceded the fragmentation of the Columbia Supercontinent. Simões et al. (2020) identified the Pedro Sara Formation (1766-1743 Ma), a felsic volcanism with alkaline affinity that is associated with the Vila do Carmo and Camaiú formations. The latter represents the major gold prospect in the region, and several occurrences have been described, for example, Eldorado do Juma and Pombas (Brito et al. 2010; Goulart and Silva 2019). The GGD contains metagranites and gneisses arranged along a wide NW-SE band. These granitoids are part of the Teodosia Suite, a high-K calc-alkaline magmatic series, aged between 1762-1749 Ma (U-Pb SHRIMP in zircon and titanite; Almeida et al. 2016; Oliveira and Lira 2019), and the Igarapé das Lontras Suite, with transitional chemistry and an alkaline trend, aged 1754 Ma (U-Pb SHRIMP, in zircon; Almeida et al. 2016). These suites represent late pulses of the Juruena plutonic-volcanic magmatism, and its volcanic equivalent composes the geological-structural association (Pedro Sara Formation; Simões et al. 2020). This domain is also composed of metavolcanic rocks (Grupo Colíder; Frasca et al. 2002) and paragneisses-amphibolites (Quatro Cachoeiras Complex; Oliveira and Lira 2019), and portions of the geological-structural association of deformed and metamorphosed supracrustal rocks.

The post-Juruena geological-structural association consists of units of the Serra da Providência bimodal magmatism (Scandolara et al. 2013 and references therein), represented by the Vila Maravilha Granite (Splendor et al. 2010; Almeida et al. 2016), and by the volcanic rocks of the Serra do Gavião Group (Oliveira and Lira 2019). These are the plutonic and volcanic members of the Serra da Providência Suite, which comprises an A2-type post-orogenic magmatism, generated in three main pulses in the NNW of the Juruena Terrane (1570 Ma, 1534 Ma and 1511 Ma). The mafic member of this event is the Mata-Matá Suite (Betiollo et al. 2005), which presents a syn-magmatic relationship with felsic members that occur in the form of dikes and sills intruded in the supracrustal rocks of the Juruena geological-structural association. Its crystallization ages (1510-1570 Ma) define the minimum age of the Vila do Carmo Group (Reis et al. 2013; Simões et al. 2020). There are also important occurrences of gold in these Mesoproterozoic units, which have a spatial relationship with medium- to low-temperature NE-SW trending ductile-brittle structures and cataclastic shear zones, and intense hydrothermal alteration, as found in the Gavião, Cento e Oitenta, Bunda da Ema and the Cava da Domingas artisanal mines (Goulart and Silva 2019; Meloni and Simões 2019; Oliveira and Lira 2019).

The Juruena Terrane is partially covered by sedimentary sequences deposited after the Neoproterozoic cratonization of this terrane. Important taphrogenic events occurred during this period. The oldest of them is represented by the Beneficente Group (1440-1100 Ma), a Mesoproterozoic-Neoproterozoic intracratonic basin, whose continental siliciclastic sequences underwent several revisions in terms of subdivision and stratigraphic positioning (e.g., Reis et al. 2013; Simões et al. 2020). Important manganese deposits have been described in their lateritized horizons, e.g, the Beneficente Mine (Albuquerque et al. 2017). A second event is related to the Alto Tapajós Group, represented by a Paleozoic intraplate passive rift basin (Toczeck et al. 2019). Its lagoon deposits (laminated siltstones and sandstones) date back to the Silurian-Devonian periods, as established by palynological analysis (Cruz 1982), and show phosphate potential, owing to their glauconite content (Reis 2006). Simões et al. (2021) have described the Igarapé Ipixuna Formation as the top of the Upper Tapajós Basin, based on a study of the provenance of detrital zircons (U-Pb LA-ICP-MS). They indicated maximum sedimentation of 161 Ma, Oxfordian age from the Upper Jurassic.

Finally, in the NNW of the Juruena Terrane, extensive lateritic-detrital covers and Pleistocene to recent sediments have been described, represented by the Salvaterra Formation (Almeida et al. 2016), and by alluvial deposits and fluvial terraces.

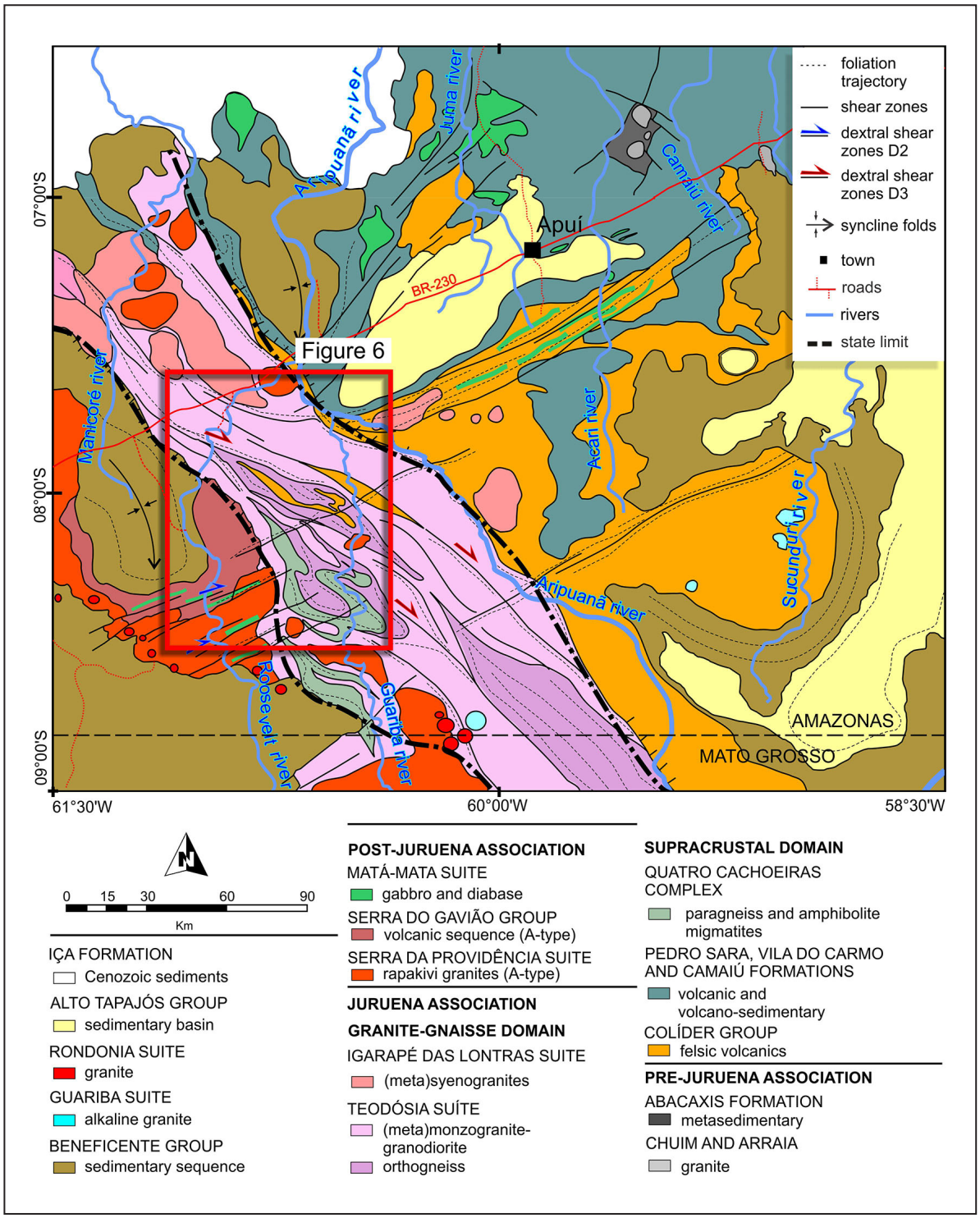

FIGURE 3. Simplified geological map of the NNW of the Juruena Terrane, SE of Amazonas State (adapted from Reis et al. 2006; Costa et al 2013; Oliveira et al. 2014; Meloni et al. 2021).

5. Results

5.1. Structural geophysical analysis

First, domains and linear features were extracted from the magnetic images, and they were numbered according to their chronology and superposition relationships. In the regional component of the magnetic anomaly, with sources with depths greater than 16 km (Figure 4A), the magnetic fabric is homogeneous and continuous with low frequency and ENE-WSW direction, arranged in alternating domains with positive and negative intensity. This magnetic fabric (L1) is superimposed and displaced by straight NW-SE (L2) magnetic discontinuities (Figure 4C). In the residual component of the magnetic anomaly, sources whose depths ranged between 16 km and 900 m (Figure 4D) do not show large-amplitude magnetic patterns, and presented attenuated L1 features. However, more intense rough magnetic textural patterns, and smooth (blurred) magnetic textural patterns with lesser magnetic intensity, single out the magnetic domains in this image. In linear magnetic

features, the L2 pattern defines a wide NW-SE band that crosses the Juruena terrane and delimits the blurred domains. Internally, this band presents features similar to fractals of shear zone structures (Figure 4D). Also in the residual component, straight and long discontinuities are singled out with high-frequency (shallow) and non-magnetic NE-SW (L3) and NW-SE (L4) discontinuities, in addition to straight magnetic NNE (L5) and semi-circular features. The latter occur in blurred domains in the eastern portion of the study area.

All these domains and features, integrated and analyzed according to a geophysical structural approach (Figure 5, Jessell et al. 1993), define the regional structural framework of the NNW of the Juruena Terrane. This pattern indicates a complex structural evolution for the region, which starts with the D1 event, represented by an EW structure (ENE-WSW) attributed to the deep basement in the region, interpreted on the basis of the L1 domains and features. This basement presents a homogeneous pattern, and does not suggest any boundary between crustal blocks; however, at shallower depths, it presents variations relative to deposition of supracrustal sequences (blurred magnetic domains) and crustal reworking and reactivation (features L2, L3, L4) (Figure 4C). Event D2 is materialized by a wide NW-SE band that crosses the Juruena terrane, superimposed on the EW structure (D1). The L2 magnetic features, with NW-SE direction and subordinately NNW-SSE, present a complex large-scale S-C pattern with dextral drag folds, enhanced at smaller depths (Figure 4D), and persistent to great depths, although attenuated (Figure 4B). Its stratigraphic position (D2) is posterior (or late) to Serra da Providência magmatism (Post-Juruena geological-structural association), whose semicircular granitic bodies intrusive in GGD (Juruena geological-structural association) are surrounded by L2 lineaments, forming a similar feature to that of the fractal of a dextral porphyroclast ellipsoid.

There are also late structural events (ductile-brittle to brittle, D3 and D4), which only respond to shallower magnetic sources (Figure 4C), associated with responses from shallow shear zones, faults and fractures that truncate and reactivate past structures. Event D3 is represented by L3 features, and non-magnetic NE-SW shear and cataclastic zones that cause dextral displacement of L2 (D2). Locally, L3 features are spatially associated with mineral occurrences and present site-specific positive magnetic anomalies (Figure 4D). Event D4 is represented by L4 features, reactivations of D2 (L2) shear

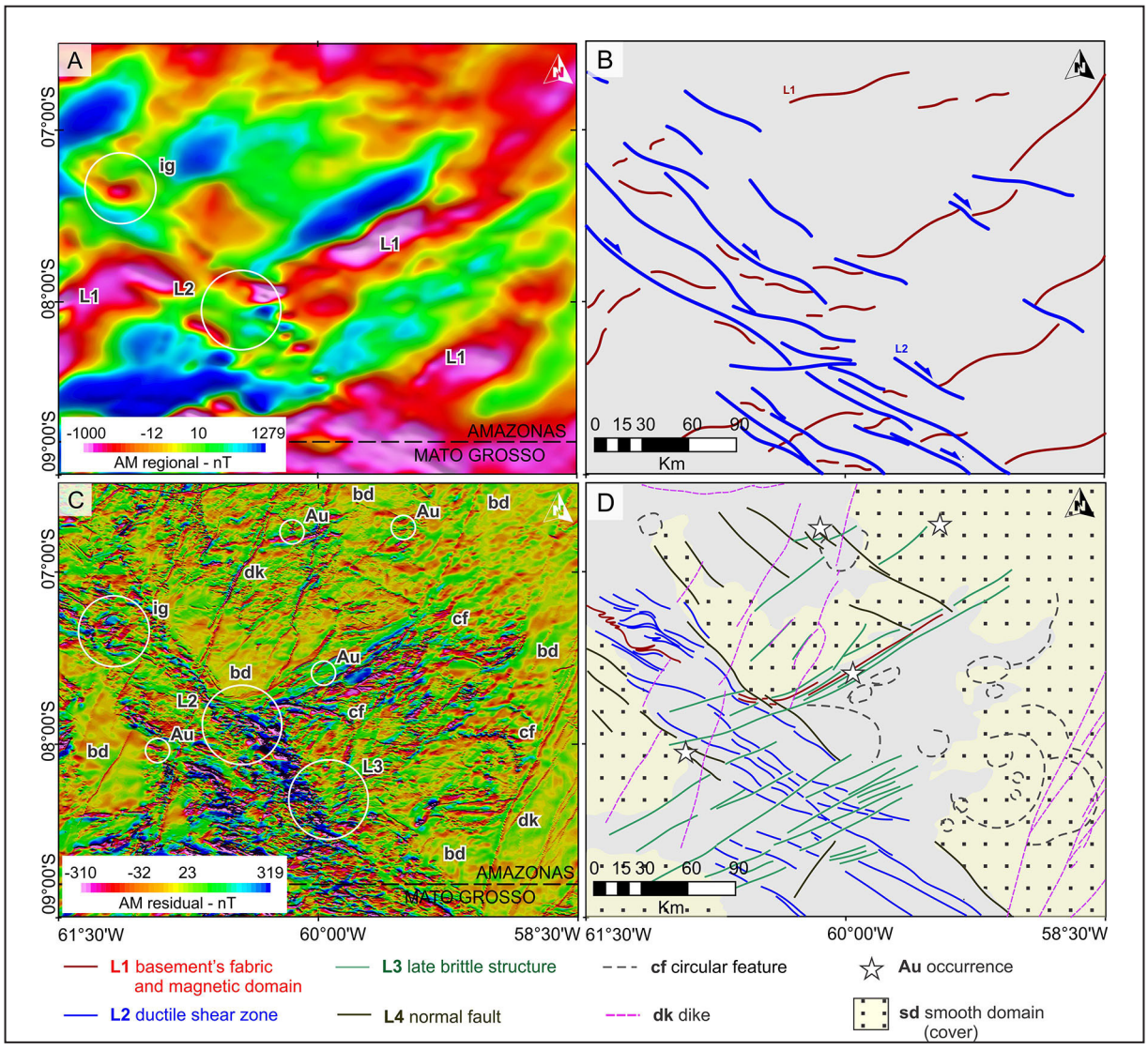

FIGURE 4. Aeromagnetic maps of regional (A) and residual (C) components, with their respective structural interpretations in (B) and (D).

zones as non-magnetic normal faults and fractures, which delimit the blurred magnetic domains, interpreted as a response of the attenuated (blurred) magnetic basement by sedimentary and volcanic sedimentary covers. Stratigraphically, the D4 structures are younger than the intracratonic Mesoproterozoic-Neoproterozoic sedimentary sequences.

Finally, there are mafic dikes with NNE-SSW direction, whose magnetic response is very well characterized by positive magnetic lineaments (L5), and ancient volcanic calderas, interpreted on the basis of semicircular magnetic features, which are truncated by D3 shear zones (L3, Figure 4D).

5.2. Structural analysis

The geological maps of the SE of the State of Amazonas (Costa et al. 2013; Oliveira et al. 2014) highlighted two main structures: the first one has NW-SE direction, and forms a high-strain band (~60 km wide, RGTB, in this study); the second is represented by subtle and spaced NE-SW shear and cataclastic zones. The high-strain band affects the GGD, controls its boundaries with the SCD of the Juruena (to the east) and Post-Juruena geological-structural associations, while the NE-SW shear zones particularly affect the Post-Juruena geological-structural association and truncate the NW-SE system. For structural and metamorphic characterization of the RGTB, geological and structural sections were made along the Guariba and Roosevelt rivers (Figure 6).

5.2.1. Roosevelt Profile (ABC)

5.2.1.1. Geological-Structural Survey

The northern stretch (AB) of the Roosevelt profile (Figure 7A) covers the GGD lithotypes of the Juruena geological-structural association while the southern section (BC) covers the lithotypes of the Post-Juruena geological-structural association.

In the GGD, coarse equigranular to porphyritic grayish hornblende-(biotite)-granodiorites to grayish biotite-monzogranites and deformed pink (micro)syenogranites, are predominant. The granodiorites and monzogranites show

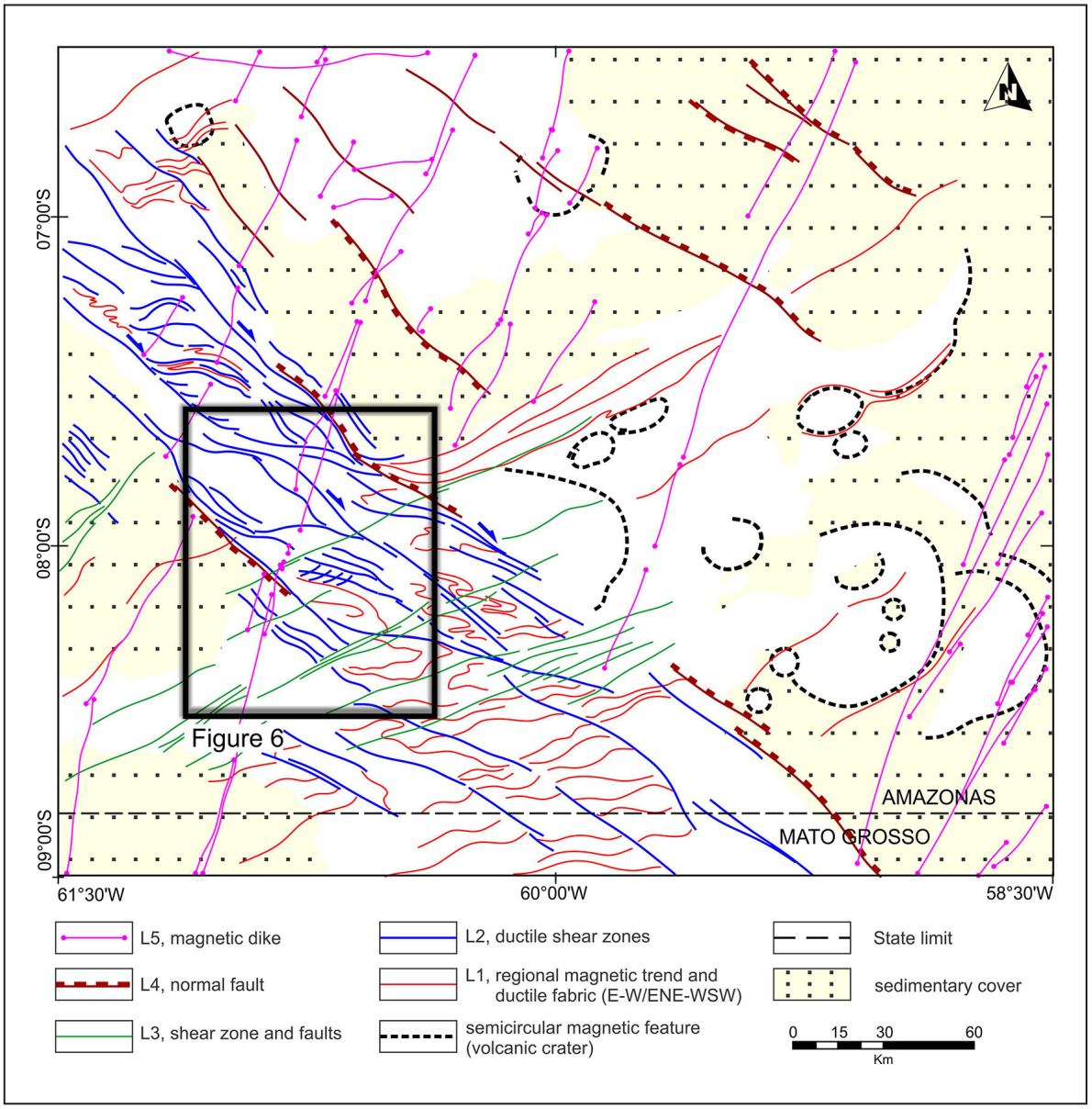

FIGURE 5. Structural geophysical interpretation of the NNW of the Juruena Terrane.

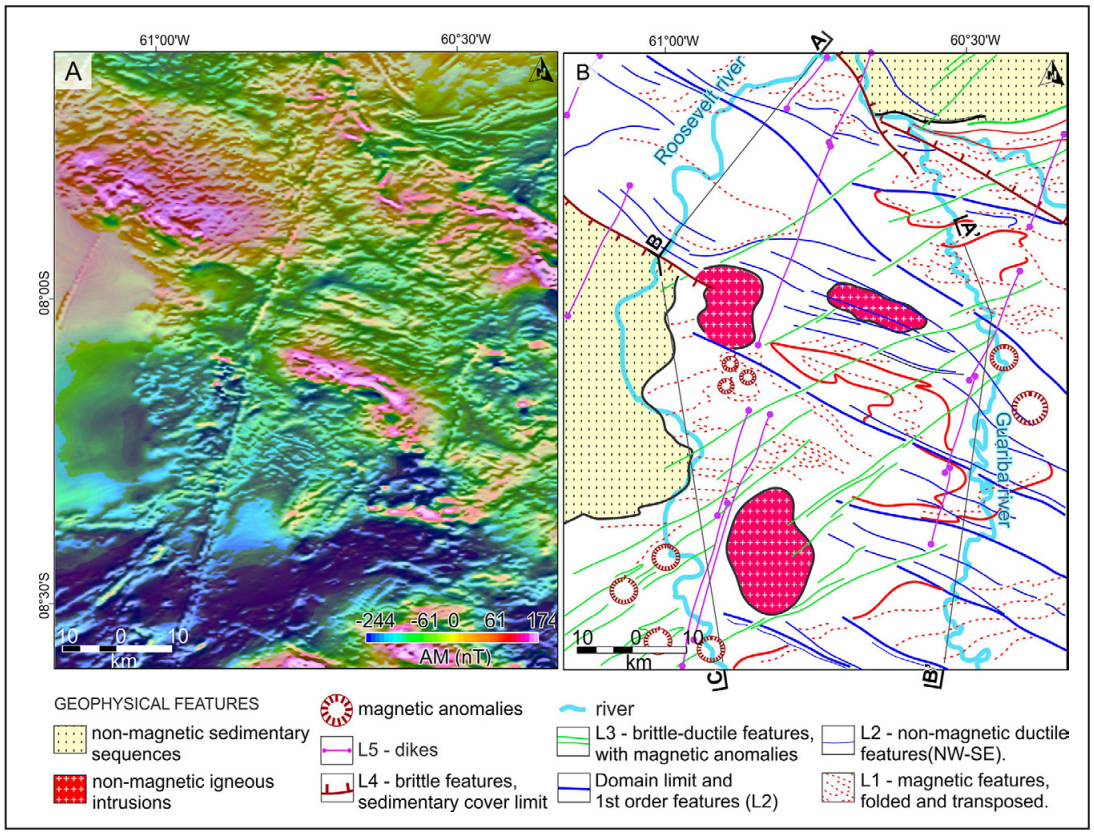

FIGURE 6. A) binary composition between magnetic anomaly (MA) and first vertical derivative of the MA (1VD.AM); B) geological and structural map interpreted in Figure 6A, highlighting magnetic responses interpreted as: intrusive bodies, sedimentary covers and magnetic anomalies. Tracings of Roosevelt (ABC) and Guariba (A'B') profiles.

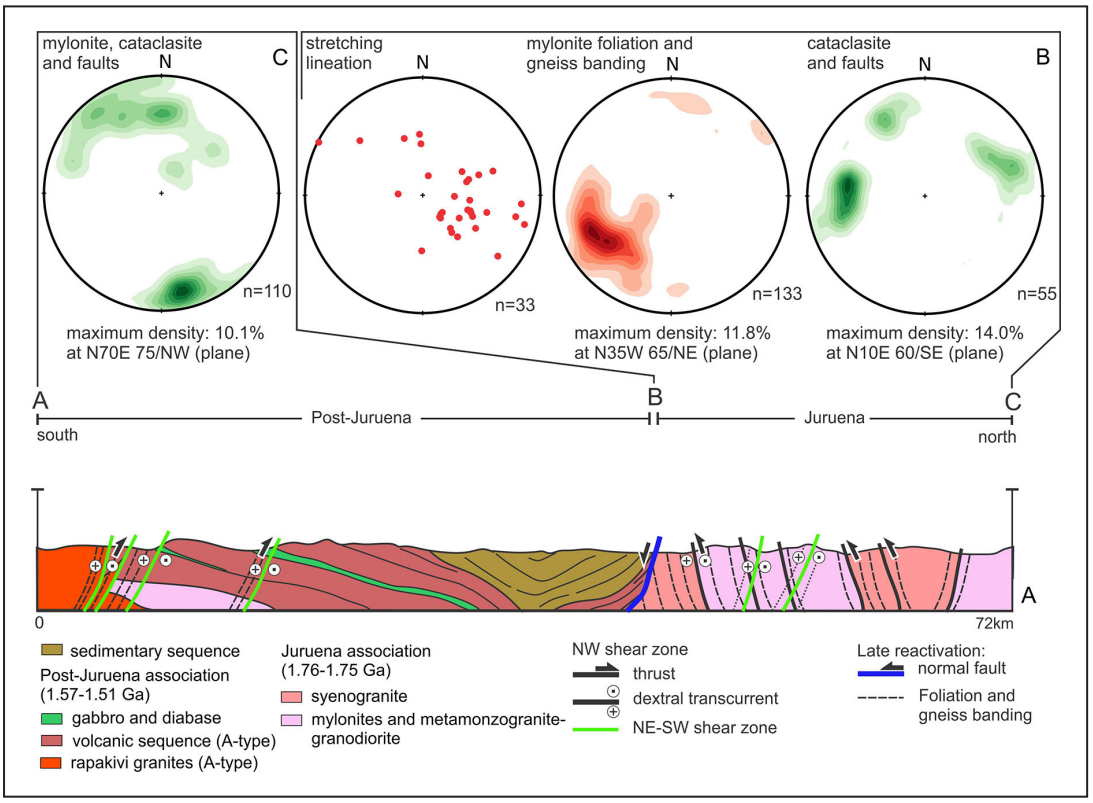

FIGURE 7. (A) Roosevelt geological profile (ABC), subdivided into north (AB), granitic gneiss of the Juruena geological-structural association, and south (BC), the Post-Juruena geological-structural association; (B) and (C) stereographic projection diagrams designed with structural data from Post-Juruena granitic gneiss domain and geological-structural association, respectively.

syn-magmatic foliation (Ssm, N70E 80/NE), defined by the alignment of tabular feldspar phenocrysts and ribbons of mafic microcrystalline aggregates (Figure 8B), also deformed according to the Ssm foliation (Figure 8A). This NNE-SSW structure is overprinted by ductile shear zones NW-SE to NNW-SSE (Figure 8C), metric and spaced, which develop mylonitic fabrics (Smi) and *augen* gneisses (Sba) in the GGD granitoids. Their planes (N20-40W 80/NE, Figure 8D) contain high-rake mineral stretching lineations (Lmi 60/N70E); therefore, these high-strain zones are defined as dextral transpressive. Syn-kinematic alkaline aplites (post-Juruena geological-structural association, Figure 8E) and mafic dykes with dextral drag folds (Juruena geological-structural association, Figure 8F) reinforce this kinematics.

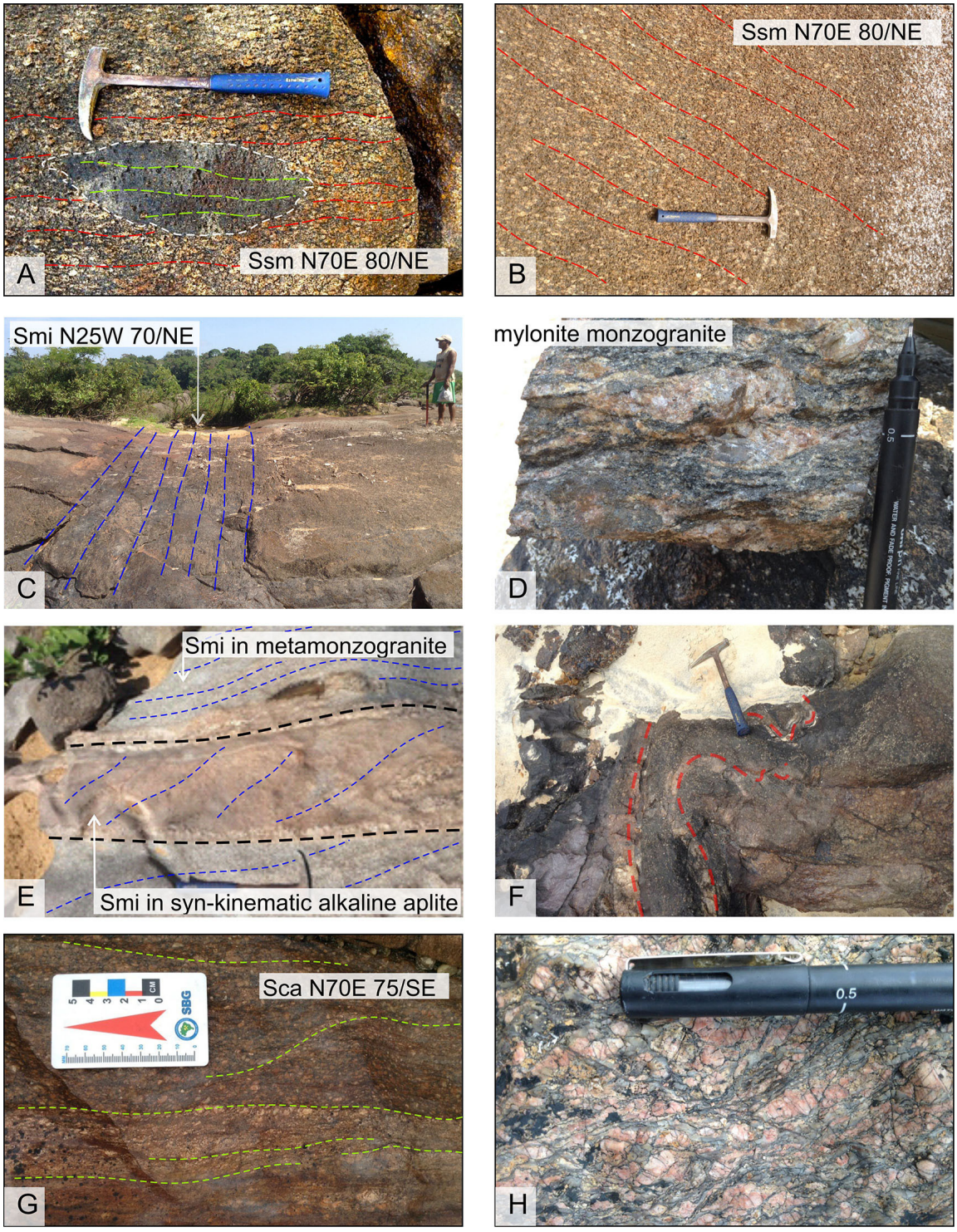

FIGURE 8. General aspects of the lithotypes from the GGD along the northern stretch of the Roosevelt profile in (A) and (B) monzogranites and autoliths with syn-magmatic foliation (Ssm); (C) ductile shear zone with NW-SE direction; (D) texture detail of augen mylonite generated in the NW-SE shear zone (mylonitic foliation, Smi); (E) NW-SE syn-kinematic syenogranitic aplite; (F) drag folds in metamafic lenses; (G) and (H) NE-SW syenogranitic cataclasite (cataclastic foliation, Sca), with intense silicification.

A third ductile-brittle to brittle structural phase affects these lithotypes. It is represented by cataclastic shear zones and faults with a general NNE-SSW direction (Figure 8G). Its cataclastic fabric has a primary attitude N70E 75/SE and a secondary N10E 60/SE and N20W 70/SW, and associated intense potassic-sericitic hydrothermal alteration (Sca, Figure 8H).

In the Post-Juruena geological-structural association, the subvolcanic, effusive and pyroclastic rocks show preserved volcanic bedding with an superimposed brittle to brittle-ductile structure, represented by breccias, faults and fractures (veins), which form cataclastic zones (Sca, N70E 75E /NW, Figure 9A,B,C). Cataclazed subvolcanic rocks are cut off by deformed mafic syn-magmatic dykes (tremolite-chlorite schists) with foliation (Sxi, N60E 70/SE) containing low-rake mineral stretching lineation (Lxis 30/N70E; Figure 9D). Along these cataclastic zones, there is intense potassification and silicification of volcanic rocks, which host gold mineralization, for example, as in Garimpo do Gavião (Oliveira and Costa 2011).

To the south of the profile, there are lithotypes of the plutonic member, and the ENE-WSW structure assumes a more ductile-brittle regime, developing dextral, metric and spaced transpressive mylonitic zones, producing ultramylonite to protomylonite fabrics in *rapakivi* granitoids. The flats (Smil N70E 80/SE) contain high-rake mineral stretching lineation (70/S80E, Figure 9E, F).

5.2.1.2. Microstructures

The GGD mylonitized granitoids associated with NW-SE shear zones show a porphyroclastic texture, with a matrix containing quartz ribbons and recrystallized plagioclase and amphibole crystals, in addition to newly-formed oriented crystals of biotite, titanite and opaque minerals, defining a pervasive foliation. Microcline porphyroclasts show undulating extinction, mantle-core structure and microfractures, which are filled with recrystallized material, suggesting reactions at high temperatures (between 500-700°C; Trouw et al. 2009) (Figure 10A). Subhedral biotite resistates are found in recrystallized aggregates of mafic minerals, reinforcing the interpretation of conditions analogous to medium to high-grade metamorphism (Passchier and Trouw 2005). *Augen* gneisses, also generated in NW-SE shear zones, show similar texture to that of ribbon

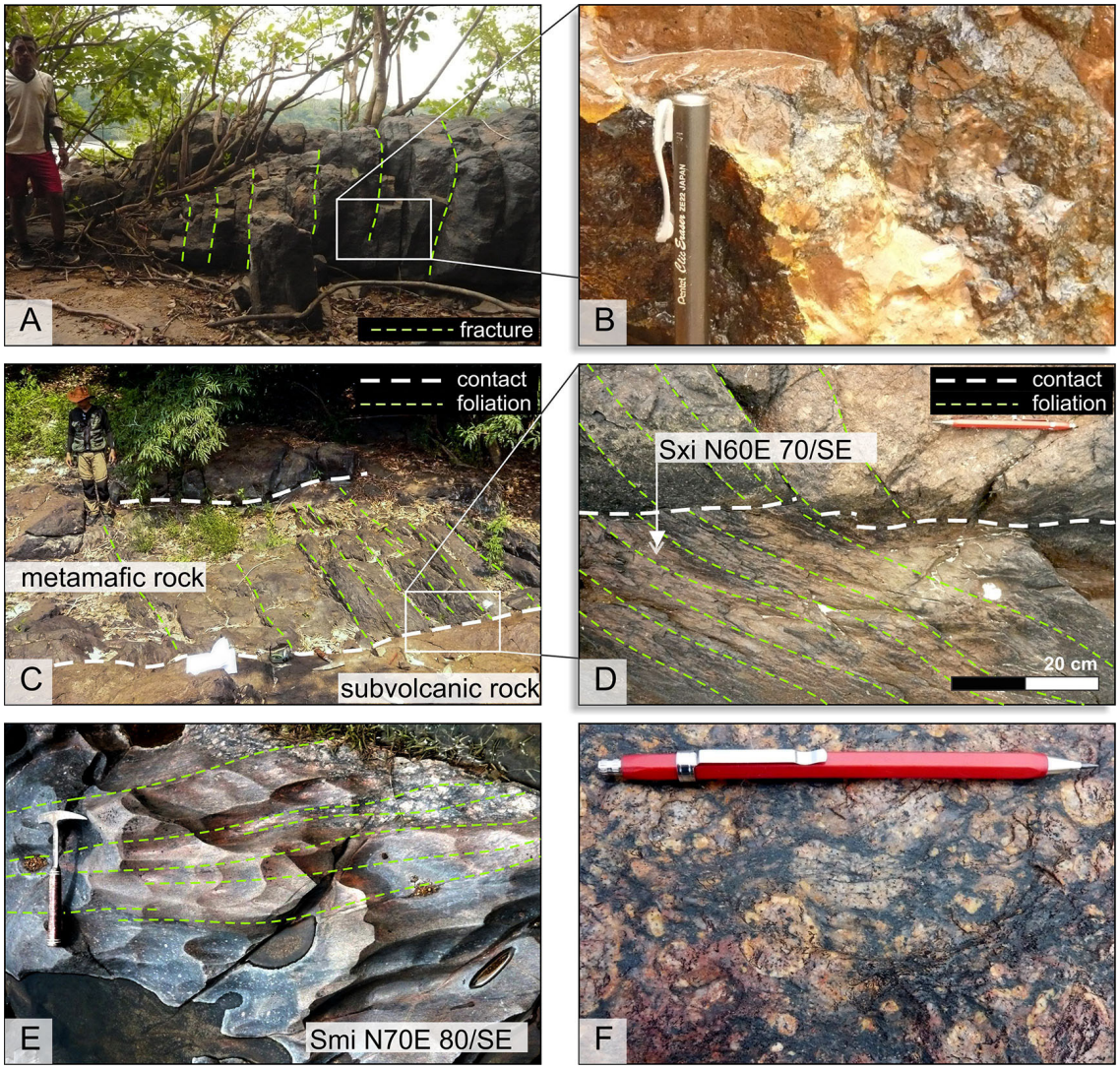

FIGURE 9. General aspects of the lithologies of the Post-Juruena geological-structural association along the southern stretch of the Roosevelt profile in (A) outcrop and (B) detail of effusive cataclastic volcanic texture; (C) outcrop and (D) detail of contact between felsic hypabyssal rock and mafic syn-magmatic dykes, which develop brittle and ductile fabrics (schistosity, Sxi), respectively; (E) outcrop and (F) detail of mylonitic-cataclastic texture (Smi) in viborgites.

gneisses, with polygonal quartz feldspathic matrix and recrystallized ribbon quartz (Figure 10B), characteristic of high-temperature mylonites (between 500-700°C; Trouw et al. 2009). Cataclastic granites, affected by NNE deformation bands, show a cataclastic fabric superimposed on a high-temperature fabric, preserved in microliths (Figure 10D). These rocks have a comminuted texture, with quartz porphyroclasts with intense crystalloplastic deformation and undulating extinction, and microfractured feldspars, in addition to intense hydrothermal alteration (Figure 10C). These microstructures are characteristic of low-temperature cataclastic and protomylonitic fabrics (<350 °C; Trouw et al. 2009).

In the post-Juruena geological-structural association, only low temperature deformation records were observed, with cataclastic ENE-WSW structure in volcanic lithotypes, as shown by rhyolitic ignimbrites and porphyritic rhyolites with primary volcanic textures superimposed by a cataclastic fabric, characterized by quartz porphyroclasts, with undulating extinction and partial recrystallization, and feldspars, fractures constituting deformation microbands with newly-formed sericite (Evans, 1988, Figure 11A) and mylonitic texture in rapakivi granites, which present comminuted porphyritic texture with quartz porphyroclasts, with intense subgrain rotation recrystallization and ribbon structures; microcline porphyroclasts show microfractures and slight undulating extinction. The porphyroclasts are surrounded by deformation microbands (Smi, Figure 11D), constituting structures such as pressure shade, whose kinematic indicators are dextral (Figure 11C). Temperature estimates are compatible with greenschist facies conditions, reinforced by the presence of tremolite-chlorite schist (deformed syn-magmatic mafic dykes) with lepidoblastic texture, defined by the planar arrangement of newly-formed chlorite and tremolite-actinolite, indicating metamorphism in the lower greenschist facies (Bucher and Grapes 2011) (Figure 11B).

5.2.2. Guariba Profile (A'B')

5.2.2.1. Geological-Structural Survey

The Guariba profile (Figure 6B) intersects lithotypes of the Juruena geological-structural association; predominantly, there are lithotypes from the GGD and, subordinately, lenses of metavolcanic rocks and migmatitic paragneisses-amphibolites from the SCD (Figure 12A). Along the profile, it can be seen that these lithotypes present deformation at different intensity levels, characterizing a low-strain north sector and a high-strain southern sector.

In the northern sector, there are isotropic monzogranites and granodiorites. However, when deformed, they show tenuous and discontinuous foliation (Sxi) N30-60W 70/NE, defined by microcrystalline hornblende, biotite and magnetite ribbon aggregates; and subparallel discrete shear zones (Smi). In this sector, there are also bands of metaquartz-trachytes and porphyritic metarhyodacites whose schistosity is defined by biotite-actinolite films, bypassing deformed quartz and feldspar phenocrysts, with attitudes ranging between N70W 78/SW and N30E 80/SE (Figure 13A).

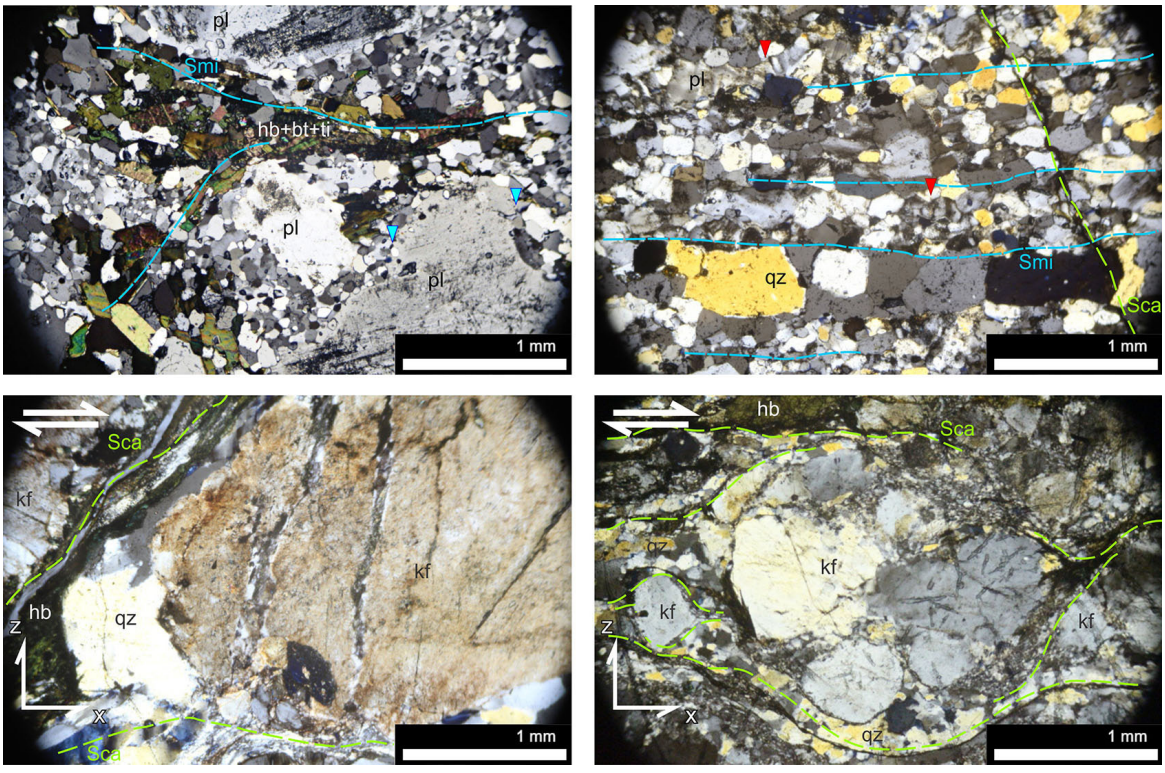

FIGURE 10. Microstructures in GGD lithotypes in (A) mantle-core structure (cyan arrow) and undulating extinction in plagioclase (pl) porphyroclasts immersed in a quartz feldspar matrix recrystallized with newly-formed mafic aggregates (hb+bt-ti) defining foliation (Smi); (B) polygonal feldspathic quartz matrix (red arrow) with recrystallized ribbon quartz (foliation, Smi); there are also microfractures (Sca) =superimposed on high-temperature fabric; (C) microcline porphyroclast (kf) whose microfractures are filled with recrystallized material, also surrounded by cataclastic microbands (Sca); there are also pressure shadows with recrystallized quartz (qz) and hornblende clasts (hb); (D) microcline porphyroclast (kf) with intense fracturing, surrounded by cataclastic flow microbands (Sca).

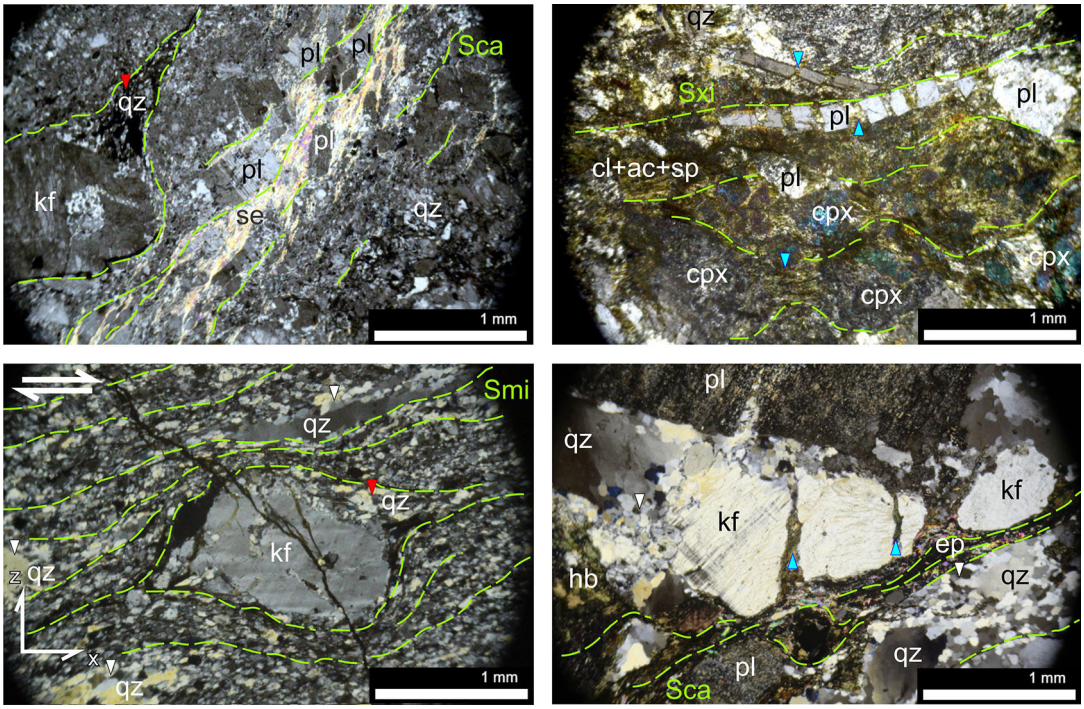

FIGURE 11. Microstructures in the lithotypes of the Post-Juruena geological-structural association in (A) hypabyssal rhyolite with microcline porphyroclasts (kf), contoured by foliation (Sca) generating a pressure shadow structure (red arrow), and plagioclase (pl) fragmented into cataclastic flows, with intense sericite alteration, set in a quartzo-feldspathic comminuted matrix; (B) tremolite-chlorite schist with plagioclase (pl) and clinopyroxene (cpx) porphyroclasts surrounded by schistosity zones and forming microboudins (cyan arrow); (C) microcline porphyroclast (kf), surrounded by foliation (Smi), generating a pressure shadow structure (red arrow), and quartz porphyroclast (qz), with intense recrystallization by subgrain rotation (white arrow), immersed in a comminuted matrix ; D) microcline (kf) and plagioclase (pl) porphyroclasts: intense fracturing, with spaces filled by recrystallized material (cyan arrow) and with intense associated hydrothermal alteration, defining cataclastic foliation (Sca).

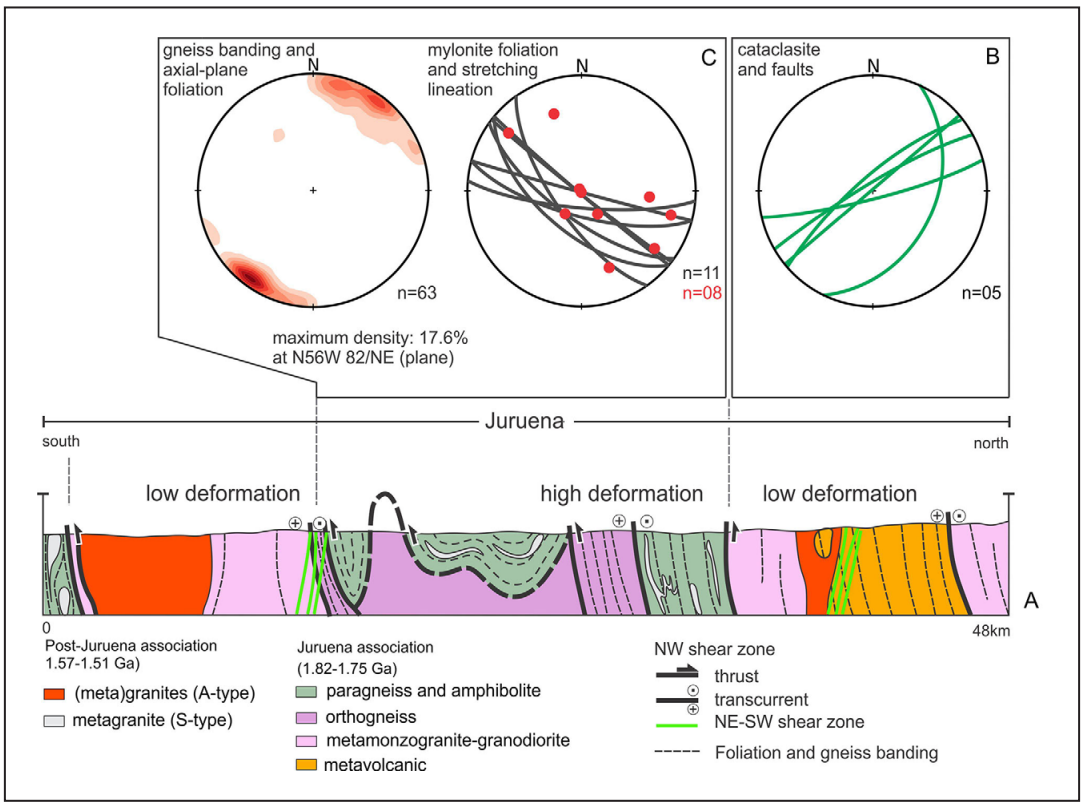

FIGURE 12. (A) Guariba geological profile (A'-B'); (B) and (C) stereographic projection diagrams designed with structural data from the low-strain (northern) and high-strain (southern) sectors, respectively.

In the southern section of the profile, there are intrusions of isotropic syenogranites (Post-Juruena geological-structural association) with metavolcanic xenoliths (Figure 13B). In the high-strain sector, metagranitoids and orthogneisses with folded bands outcrop with boudinated amphibolite lenses (Figure 13C), which form a NW-SE fabric represented by continuous axial plane (Spa) and mylonitic (Smi) foliations, with attitude N40W 80/NE (Figure 13C).

Along with the orthogneisses, there are paragneiss bands with very thin banding defined by the alternation of quartz-feldspar layers and muscovite-biotite-sillimanite levels, interspersed with amphibolite levels, SCD of the Juruena geological-structural association. This folded and refolded banding develops a transposition fabric with N30W 80/SW attitude planes (Figure 13F), where one can single out isoclinal folds with an subhorizontal axis in the NW-SE direction, which are superimposed by asymmetric folds with a subvertical axis (Figure 14A, B). These paragneisses show layers of stromatic migmatitic metatexites (Figure 13E), with leucosomes parallel to the gneiss band, showing boudins and ptigmatic folds that suggest dextral transpressive kinematics for this system (Figure 14C, D). There are small leucogranite stocks and dykes associated with paragneisses.

Along the entire profile, a second generation of structures with NE-SW direction is developed in brittle and brittle-ductile regimes in shear, fault and fracture zones. These features are spaced and develop cataclastic to mylonitic (Sca) fabrics with general attitude N30E 70/SE, truncating the predominant NW-SE structure.

5.2.2.2. Microstructures

The metagranitoids and orthogneisses show a porphyroclastic texture, with a thick polygonal matrix, feldspar porphyroclasts with undulating extinction, wedged twins and mantle-core structure (Figure 15A) recrystallized quartz ribbons (Figure 15B) and microstructures that characterize high-temperature deformation (>600°C; Passchier and Trouw 2005).

The microstructures and mineral associations of paraderived rocks show two metamorphic phases associated with a progressive deformation event. The first metamorphic phase (M1) is characterized by high-temperature and low-pressure metamorphic paragenesis, upper amphibolite facies, composed of biotite, and andalusite, sillimanite, cordierite,

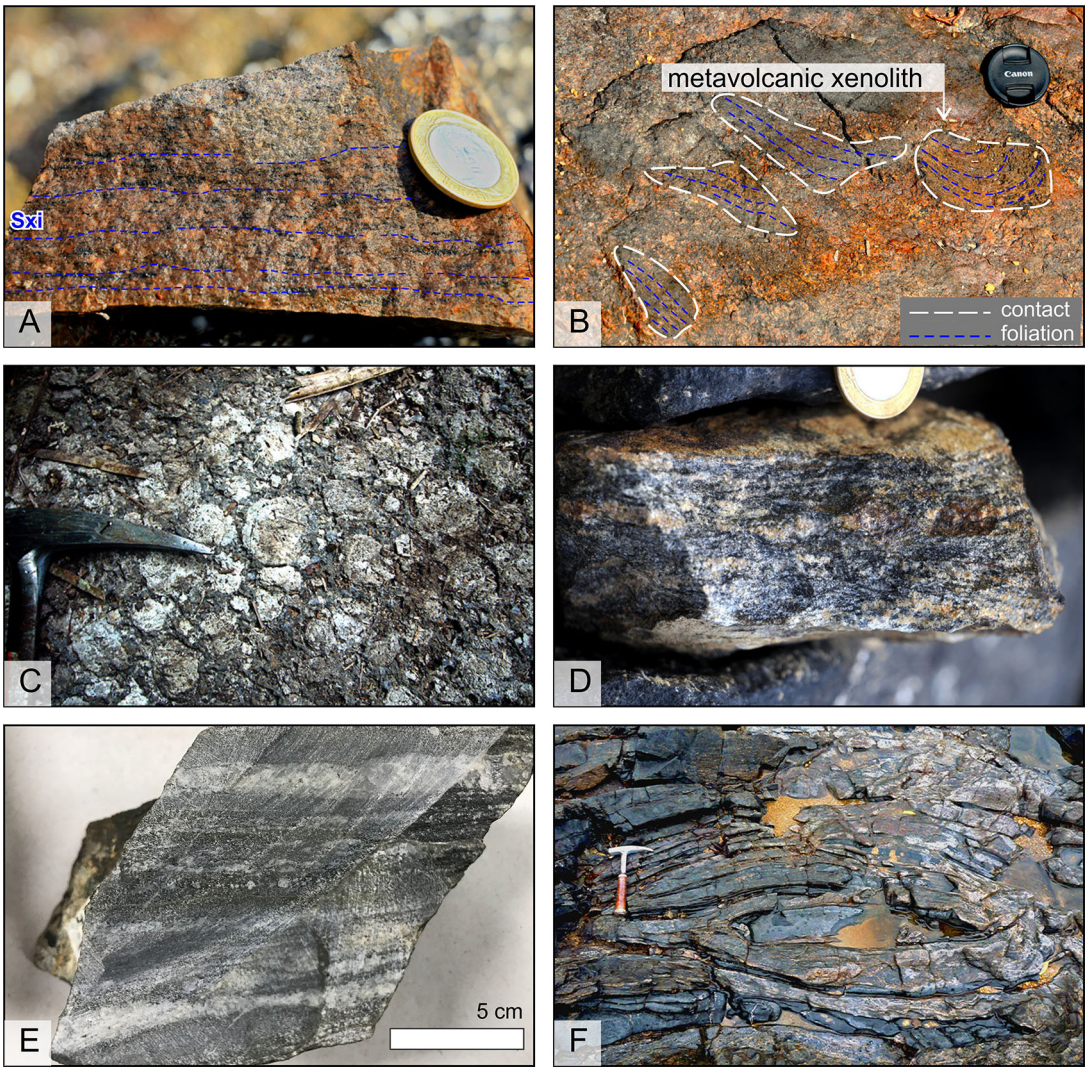

FIGURE 13. General aspects of the lithotypes along the Guariba profile in (A) Colider metarhyodacite whose schistosity (Sxi) is defined by deformed mafic minerals and phenocrysts aggregates; (B) metarhyodacite xenolith in syenogranite; (C) detail of rapakivi granite textures (viborgite); (D) migmatitic orthogneiss; (E) paragneiss (metapelite) migmatite; (F) folded paragneiss and amphibolite.

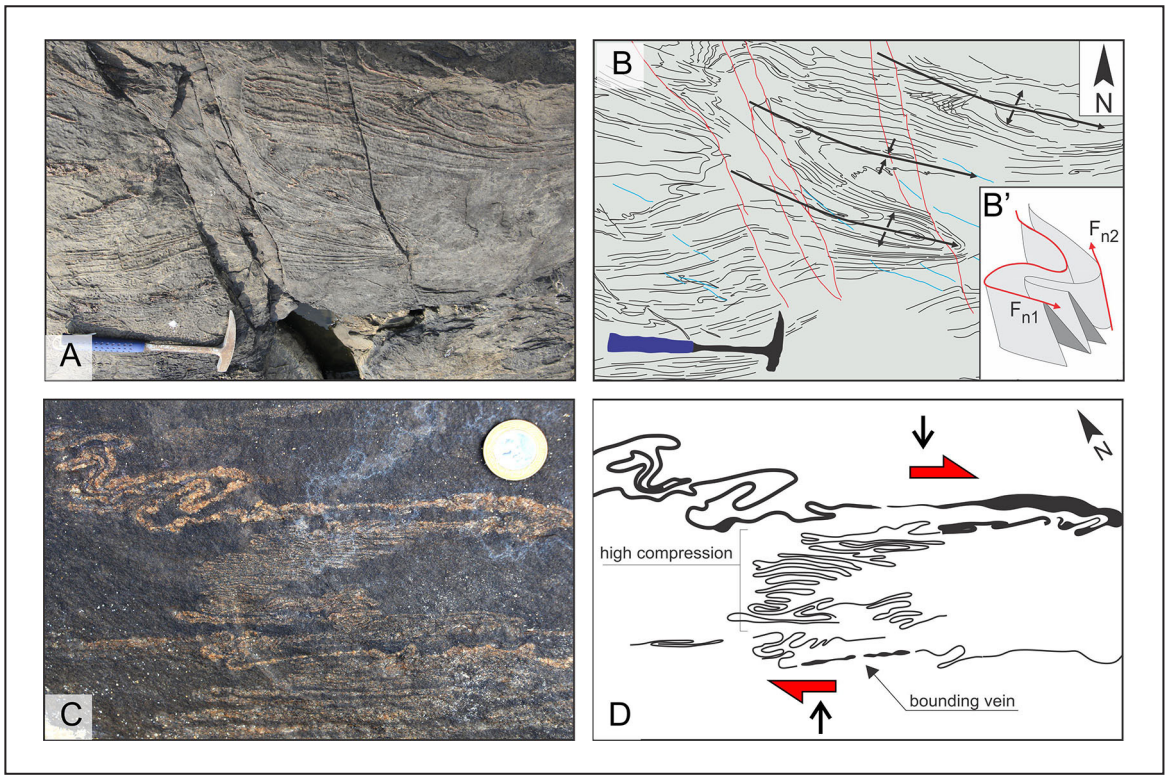

FIGURE 14. (A) outcrop of stromatic metatextite migmatitic paragneisses; (B) cartoon highlighting the structure of these migmatites, with a complex refolding pattern (B'); (C) detail of ptigmatic folds; (D) cartoon highlighting this structure and its indicators of dextral transpressive kinematics.

±garnet (Figure 15C; Bucher and Grapes 2011), which has *in situ* fusion features, resulting from the migmatization process (Figure 15D). The second metamorphic phase (M2) is in the greenschist facies (retrograde), defined by the overgrowth of biotite and muscovite in crenulation cleavage planes.

Superimposed on this fabric, quartz crystals with subgrain rotation recrystallization (Figure 15E) and microfractured feldspar grains indicate low-temperature deformation (350-400°C, Passchier and Trouw 2005). Asymmetric recrystallization tails (Figure 15F) indicate dextral kinematics for this structure.

6. Discussion

6.1. Structural and metamorphic evolution of the Roosevelt-Guariba Transpressive Belt

The structural analysis of outcrops and the microtectonic study allowed to characterize the high-temperature and medium to low-temperature sectors, possibly related to the partition dynamics in the dextral transpressive deformation. The description of these sectors makes up the structural and metamorphic history of the RGTB (Figure 16A).

6.1.1. Past structures (D1)

The first generation of planar structures (S1) encompasses syn-magmatic foliations (Ssm) observed in the medium and low-temperature sector of the RGTB in the lithotypes of the GGD. The Ssm foliation has a N70E 80/SE attitude, predominantly described in the northern section of the Roosevelt profile. In the high-temperature sector, these structures are relicts and were almost completely obliterated by later deformation phases; they are found locally, for example, in mesoscopic-scale fold hinges (D2). These structures (S1) compose the D1 event in the NNW of the Juruena Terrane, showing low-strain intensity that can be associated with the distance of the deformational front of the Juruena orogen. Thus, D1 is the result of a syn- to late-magmatic deformation, with ENE-WSW trending (Figure 19A), whose intensity decreases from south to north, and is partially transposed by later events (Figure 17A) and correlated with the regional ductile fabric of the Juruena Terrane in the Colniza region, Mato Grosso (Ribeiro and Duarte 2010; Scandolara et al. 2017).

6.1.2. Second generation of structures (D2)

The structures generated in event D2 are shear zones, foliations, bandings, tight folds to isoclinals and boudins, which form a wide NW-SE band and are the main structural feature in the NNW of the Juruena Terrane. The S2 foliations (Smi, Sba and Spa) have a general NW-SE direction, from high dip angles to NE. In the Roosevelt profile, the shear zones have medium and high temperature, are developed in granitoids of the GGD, with Smi (N35W 65/NE) defined by newly-formed biotite-amphibole-titanite-magnetite ribbons with a partially recrystallized matrix with quartz ribbons and microcline porphyroclasts with core-mantle structures. In the Guariba profile (southern section), isoclinal and tight folds with Spa (N56W 80/NE) are predominant, with boudinated flanks, and broken by shear zones. Migmatitic melts are also common, and they generate stromatic metatexite.

When the D2 fabric affects the granitoids from the GGD, it generates mylonitized orthogneisses, which present

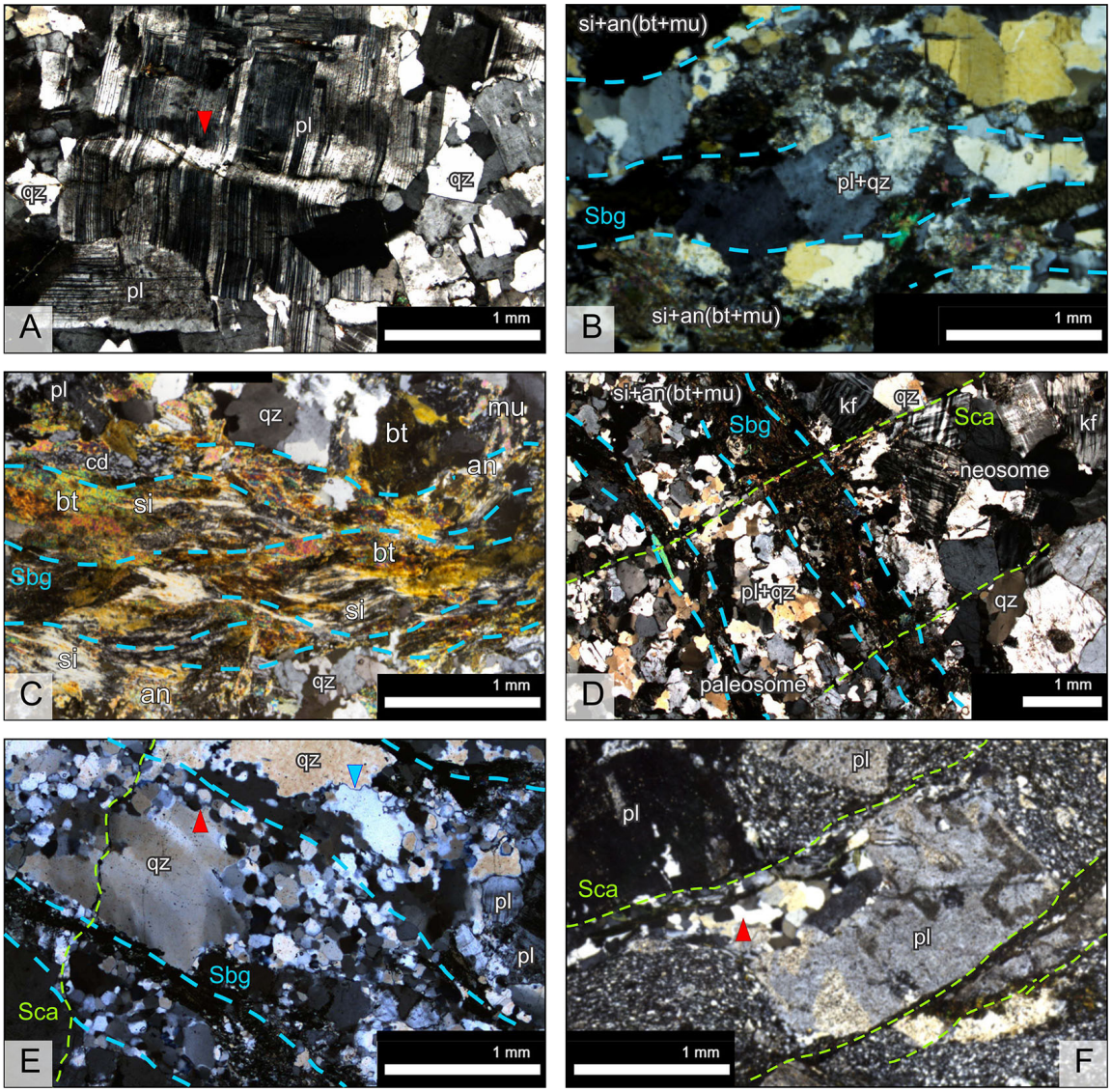

FIGURE 15. Photomicrographs showing microstructures and metamorphic mineral associations of lithotypes along the Guariba profile. (A) plagioclase porphyroclast (pl) with deformed twins (red arrow) in a polygonal quartzo-feldspathic matrix; (B,C) paragneisses with mineral association compatible with high-temperature and low-pressure conditions (M1 – pl-si-an-cd±grn) and retrometamorphic greenschist (M2 – bt-ms), well-defined foliation (Sbg); (D) contact between quartzo-feldspathic neosome and paleosome, which presents alternating bands (Sbg) sillimanite+andalusite (biotite+muscovite) and plagioclase+quartz; (E) quartz with intense subgrain rotation recrystallization (red arrow); (F) fractured plagioclase porphyroclast, with a domino structure, defined by cataclastic foliation (Sca).

microstructures typical of high-temperature mylonites (10A, B, 15A; Trouw et al. 2009), indicating metamorphic conditions compatible with upper amphibolite-to-granulite facies. By comparison, in the lithotypes from the SCD, it generates finely banded paragneisses (0.05–1 mm) with alternating levels of newly-formed biotite, sillimanite, and andalusite, cordierite, garnet, and quartz-plagioclase with polygonal recrystallization and migmatitic fusions (15B, C, D). In these rocks, there are two superimposed metamorphic mineral associations linked to D2. The first association is composed of biotite, sillimanite-andalusite, cordierite, ±garnet (M1) and defines conditions of the upper amphibolite-to-granulite facies (Winkler 1979); the second represents a retrometamorphism composed of biotite-muscovite (M2) developed in upper greenschist to amphibolite facies (Winkler 1979). Thermobarometric data of paragneisses and amphibolites from the Quatro Cachoeiras Complex confirmed conditions of upper amphibolite to granulite facies, with high temperature, >700°C, and medium pressure, 3.3 to 6 kbar. For retrometamorphism, there were lower amphibolite facies conditions, with moderate-temperature, approximately 550°C, and low-pressure, 1 to 3 kbar (Lisboa 2019). Stromatic metatexites have a complex structure with F2 folds, with isoclinal rootless folds (F1) and asymmetric F2 folds associated with dextral transpressive shear zones, suggesting deformational phases in a progressive event (Figure 14). This finding suggests that this plot is the result of superposition of deformational phases in a progressive event, D2a (M1) and D2b (M2). Along the RGTB, the granitoids of the Post-Juruena geological-structural association intrusive in the GGD are oriented in agreement with the NW-SE (D2) structure. When deformed, they present intense structuring on their edge, pervasive

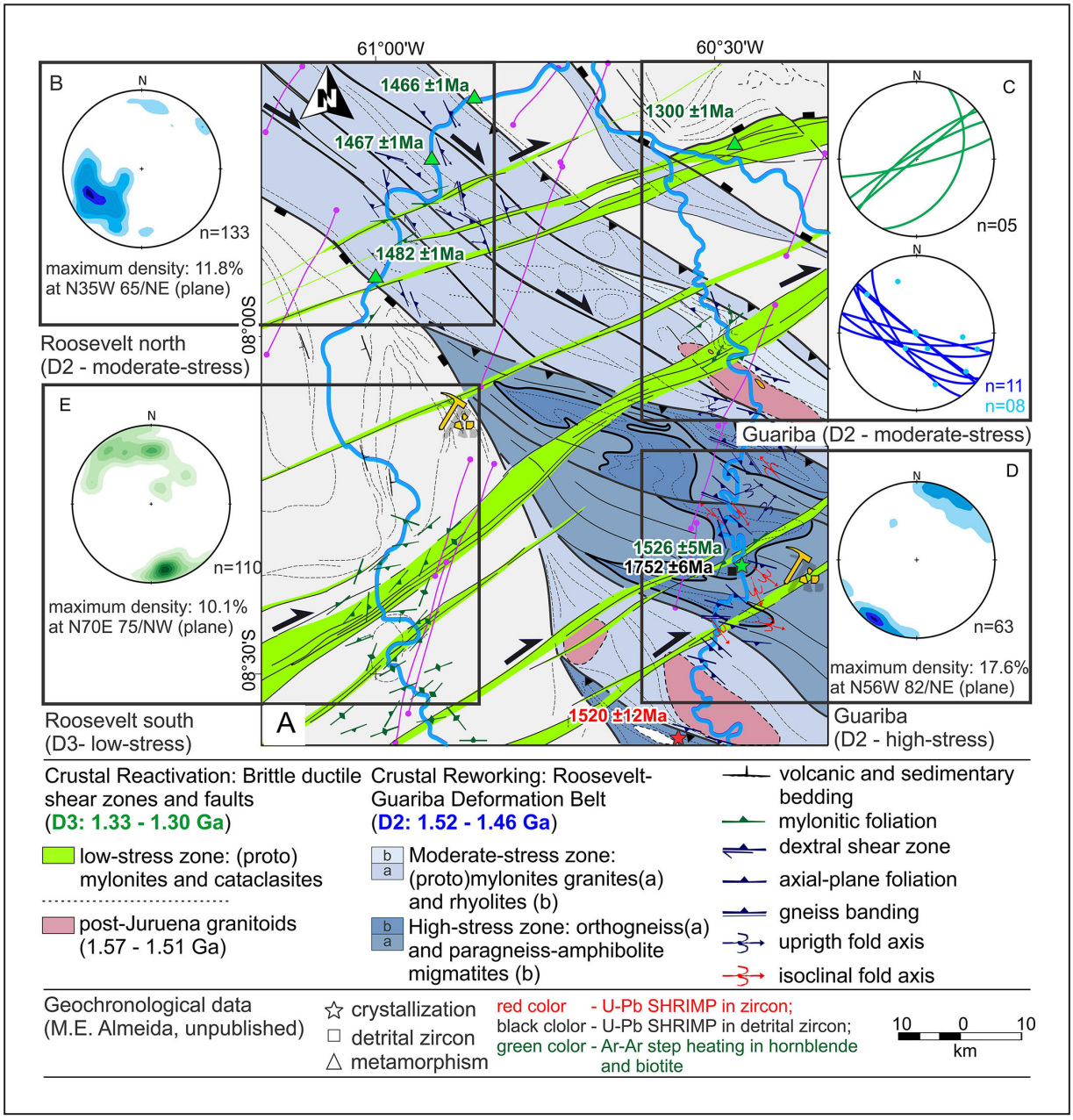

FIGURE 16. (A) Structural map between the Roosevelt and Guariba rivers, NNW of Juruena Terrane, highlighting the D2 structure - Roosevelt-Guariba Transpressive Belt (RGTB), with zones of high tectonic stress (southern Guariba) and moderate stress (northern Roosevelt and northern Guariba)); and D3 structure – shear zones and faults, which present low tectonic stress (southern Roosevelt); stereographic diagrams for structures D2 (blue tones) and D3 (green tones) referring to the northern (B) and southern (E) Roosevelt and northern (C) and southern (D) Guariba sectors. (Geochronological data compiled from Almeida M.E., unpublished written communication).

Smi and Sag, while the nuclei show slight or isotopic deformation (Figure 13C). Also, there are syn-kinematic aplitic syenogranite dykes in D2 shear zones (Figure 8E).

Recent geochronological data by Almeida et al (in prep.) show that the sedimentary protoliths of the paragneisses (metapelites) of the Quatro Cachoeiras Complex, along the Guariba River, have maximum sedimentation age of 1752 Ma (U-Pb SRHIMP in zircon) and age of the M1 metamorphic peak (upper amphibolite-to-granulite facies) ranging between 1520-1526 Ma, provided by the dating of stromatic metatexitic paragneiss and S-type leucogranite plugs (U-Pb SRHIMP in zircon). Those data also show that orthoderived mylonites and protomylonites generated in event D2 (RGTB), located in the northern section of the Roosevelt profile, presented Ar-Ar plateau ages (step heating) of 1482 Ma (hornblende), 1467 Ma (muscovite) and 1466 Ma (biotite).

6.1.3. Third generation of structures (D3)

Structures developed during the third deformational event (D3) are subtle on the outcrop scale and are spaced on the metric to decimetric scale. Its ductile-brittle to brittle fabric (S3 is associated with low-temperature NE-SW shear zones and cataclastic bands, represented by fracture cleavage, cataclastic flows, faults, fractures and veins. Along the RGTB, features generated in event D3 truncate the NW-SE D2 fabric. In the Guariba profile,

metavolcanic lenses from the SCD show an S2 trajectory drawing dextral drag folds associated with D3 shear zones.

In the lithotypes of the Post-Juruena geological-structural association, the main D3-related NE-SW (ENE-WSW) structuring, as shown by the lithotypes along the Roosevelt profile in its southern sector, the volcanic rocks show a brittle structure (fractures, cataclastic flow and fracture cleavage) while the plutonic rocks show a ductile-brittle structure (mylonitic foliation). The felsic volcanic and subvolcanic lithotypes present typical low-temperature microstructures, with a dynamically recrystallized matrix, fractured phenocrysts and dextral deformation microbands, filled with sericite (alteration of feldspar clasts) and dynamically recrystallized quartz (Figure 11A). Meanwhile, mafic lithotypes show a metamorphic mineral association of greenschist facies constituted by chlorite, tremolite-actinolite, in metadiabase (Figure 11B). In the plutonic member, kinematic indicators define dextral transpressive shear zones (Figure 11C).

The arrangement of the lithotypes of the geological-structural association, generated in different and synchronous crustal levels, suggests that deformed and juxtaposed lithotypes are formed during D3. There is also intense hydrothermal alteration along these NE-SW shear zones, generating potassium metasomatism represented by the mineral phases epidote-silica-fluorite-hematite-pyrite. These alteration zones have an important relationship with gold mineralizations hosted in volcanic rocks of the Serra do Gavião Group (Garimpo do Gavião).

6.1.4. Late-reactivation structures (D4)

A last set of structures joining normal faults and fractures in the NW-SE and NNE-SSW directions, with subvertical dips, control the contact between the Mesoproterozoic-Neoproterozoic and Paleozoic sedimentary successions of the Beneficente (Almeida et al. 2016; Reis et al. 2013) and Alto Tapajós (Reis 2006; Toczeck et al. 2019) groups, and the lithotypes of the Juruena geological-structural association. They are reactivation structures, defining D4 as a late event in the NNW of the Juruena Terrane. In regional structural geophysical analysis, L4 lineaments are interpreted as normal faults generated especially from L2 lineament reactivations, which limit blurred magnetic domains, which coincide with the exposures of sedimentary covers.

6.2 Implication of the structural framework of the NNW--Juruena Terrane in the evolutionary context of the Rondônia-Juruena Province

Evolutionary models of the Juruena Terrane (Scandolara et al. 2017; Duarte et al. 2019; Rizzotto et al. 2020a, 2020b and cited references) admitted that the NNW sector of the Juruena Terrane represents a volcanic-sedimentary basin with a basement chronologically correlated with the Tapajós Crust, a Pre-Juruena geological-structural association, although they have described the NW-SE structure of this region as being generated during the architecture of the Juruena Terrane.

As for the nature of this volcanic sedimentary basin, the intensity of the EW regional deformation of the Juruena Terrane (D1) decreases from southwest to northeast, and the supracrustal sequences of the SCD from late-Orosirian to Statherian age are free from tectonic stress, and preserve their primary structure (Reis et al. 2013; Simões et al. 2020). This fact suggests that the NNW of the Juruena Terrane represents the foreland region in the Juruena Orogen (Scandolara et al. 2017), with the Tapajós Crust extending to the west, beyond the limit established in the models of geochronological provinces (Santos et al. 2000; Cordani and Teixeira 2007). Simultaneously, the base of this basement was reworked and intruded by plutonic bodies, which constitute the GGD, as shown by data from isotopic geochemistry and inheritance ages (Almeida et al. 2016) (Figure 17A).

The RGTB is the main structure of the NNW of the Juruena Terrane, a dextral transpressive shear zone system, which reaches depths greater than 16 km and is superimposed on the Juruena Terrane's EW regional structure (ENE-WSW). This transpressive belt controls geotectonic compartments in the region, juxtaposing temporally correlated plutonic units (GGD) and volcanic and volcanic-sedimentary successions (SCD) of the Juruena geological-structural association. The RGTB-affected lithotypes developed high-temperature mylonitic fabrics (orthoderived from the DGD) and metamorphism compatible with upper amphibolite facies, with migmatitic portions and small anatectic bodies (paraderived from the SCD).

The RGTB characterizes a tectonic event of intracontinental crustal reworking in the Juruena Terrane, later architecture of the Juruena geological-structural association, as evidenced by syn-kinematic syenogranitic aplites (Post-Juruena geological-structural association) along NW-SE shear zones and their superposition relationship with the EW regional structure of the Juruena Complex, Colniza Region – NW of Mato Grosso (Ribeiro and Duarte 2010), where it is represented by the Canamã Fault and the Arinos-Aripuanã Lineaments (Araújo et al. 1978; Silva et al. 1980, 1974). Paragneisses and leucogranites from the Jamari Terrane, in the central-eastern region of Rondônia, which presented Mesoproterozoic age of metamorphism and crystallization, respectively, are also correlated with this event (Payolla et al. 2003a, 2003b; Quadros et al. 2011).

The driving force for this Calymmian tectono-thermal event is attributed to distal stresses around the continent, such as the Cachoeirinha (Ruiz et al. 2004), the Rondoniano-San Ignacio (Bettencourt et al. 2010) and the Içana (Almeida et al. 2013) orogens. Another factor that contributed to the development of this intracontinental event was the Serra da Providência magmatism (1570-1510 Ma, Post-Juruena geological-structural association), with common heat and fluid input in post-collisional A2-type magmatism, owing to its association with the rise of the lithospheric mantle through the process of delamination of the accretionary crust and/or slab breakoff (Scandolara et al. 2013 and references therein) (Figure 17B).

The cratonization of the Juruena Terrane is marked by the development of the Beneficente Sedimentary Basin (Reis et al. 2013), a process of broad intracratonic taphrogenesis that covered the Juruena Terrane between 1.40 and 1.00 Ga (Figure 17C).

Other generations of structures are singled out: both D3 and D4 characterize crustal reactivation events. D3 is spatially associated with metasomatism and gold mineralization in the region (Figure 17C), and D4 is represented by late normal faults that particularly reactivate NW-SE structures (D2), controlling the development of Paleozoic basins (Toczeck et al. 2019) and shaping the landscape (Figure 17D).

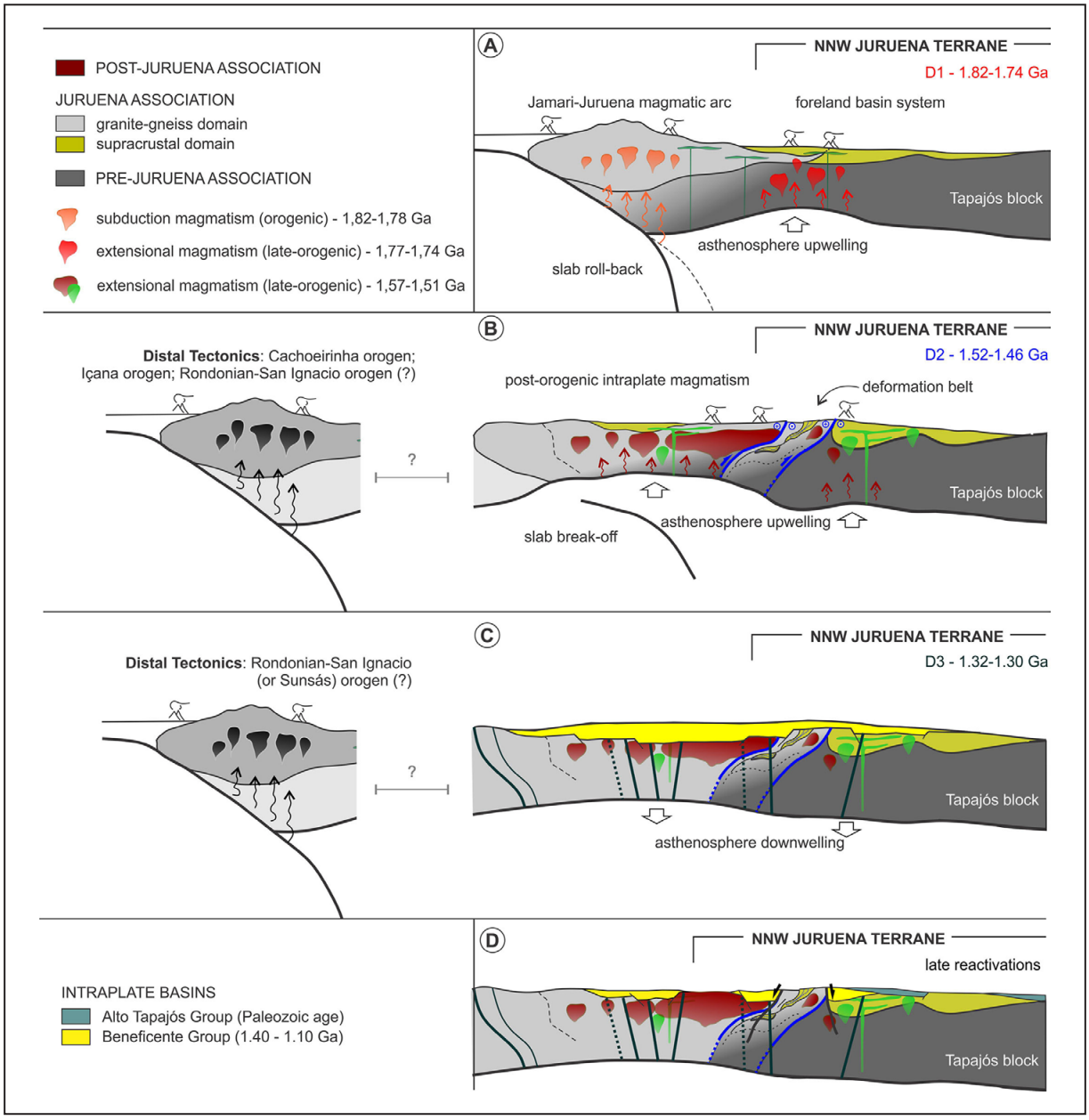

FIGURE 17. Schematic evolutionary model of the Juruena Orogen, considering the structural framework of the NNW portion of the Juruena Terrane, southeastern Amazonas State. (A) event D1: architecture of the Juruena and Jamari magmatic arcs, highlighting two phases of magmatism; (B) event D2: orogenic collapse and intracontinental crustal reworking, whose stresses are reflexes of distal orogeny; (C) event D3: crustal reactivations and reworking attributed to reflexes of the Rondoniano-São Inácio Orogen (Bitencourt et al., 2010) or the Sunsás orogenic cycle (Santos et al. 2008); and (D) late reactivations: gravitational neotectonics, constituting horst-graben systems that shape the current landscape.

7. Final remarks

The multiscale analysis of the RGTB using mapping and structural interpretation enabled the interpretation of the structural framework of the NNW of the Juruena Terrane in the SE of Amazonas. In addition, it identified the relative and absolute chronology of its deformational and thermal events. Using aeromagnetic data and its filtered products to interpret subsurface deformation, proved to be invaluable in this region, which has few rocky exposures and restricted access, thus supporting the conclusions presented below.

The structural framework of the NNW-Juruena Terrane could be redesigned with the aid of regional structural geophysical analysis (Jessel and Valenta 2007), based on interpretations at different crustal levels that singled out several superimposed deformational events (D1, D2, D3, D4; Figure 18). The structural analysis of outcrops and the microstructural study validated this regional interpretation, and defined the RGTB as a continental-scale tectonic feature generated by event D2. It was represented by a system of transpressional-dextral ductile shear zones, generating mylonites and migmatitic gneisses, with crystallographic features and metamorphic mineral assemblages compatible with upper amphibolite facies, under high-temperature and medium-pressure conditions (Lisboa 2019; Oliveira 2016). Internally, the NW-SE structure of the RGTB (D2) partially obliterates the EW regional structure of the Juruena Terrane (D1) and is truncated by NE-SW structures (D3). The latter is

represented by spaced brittle and ductile-brittle shear zones, which served as conduits for hydrothermal fluids, which are related to the major occurrences of gold in the region, e.g., Gavião mine.

In the NNW of the Juruena Terrane, event D1 is represented by a preexisting deep basement structure, correlated with the architecture of the Juruena Terrane (DE1). The structure (D1) is not found in the lithotypes of the Juruena Supracrustal Domain, and it is represented only by relict features (gneiss banding and syn-magmatic foliation) present in the Juruena Granitic Gneiss Domain, indicating attenuation of the intensity of the D1 deformation from SE

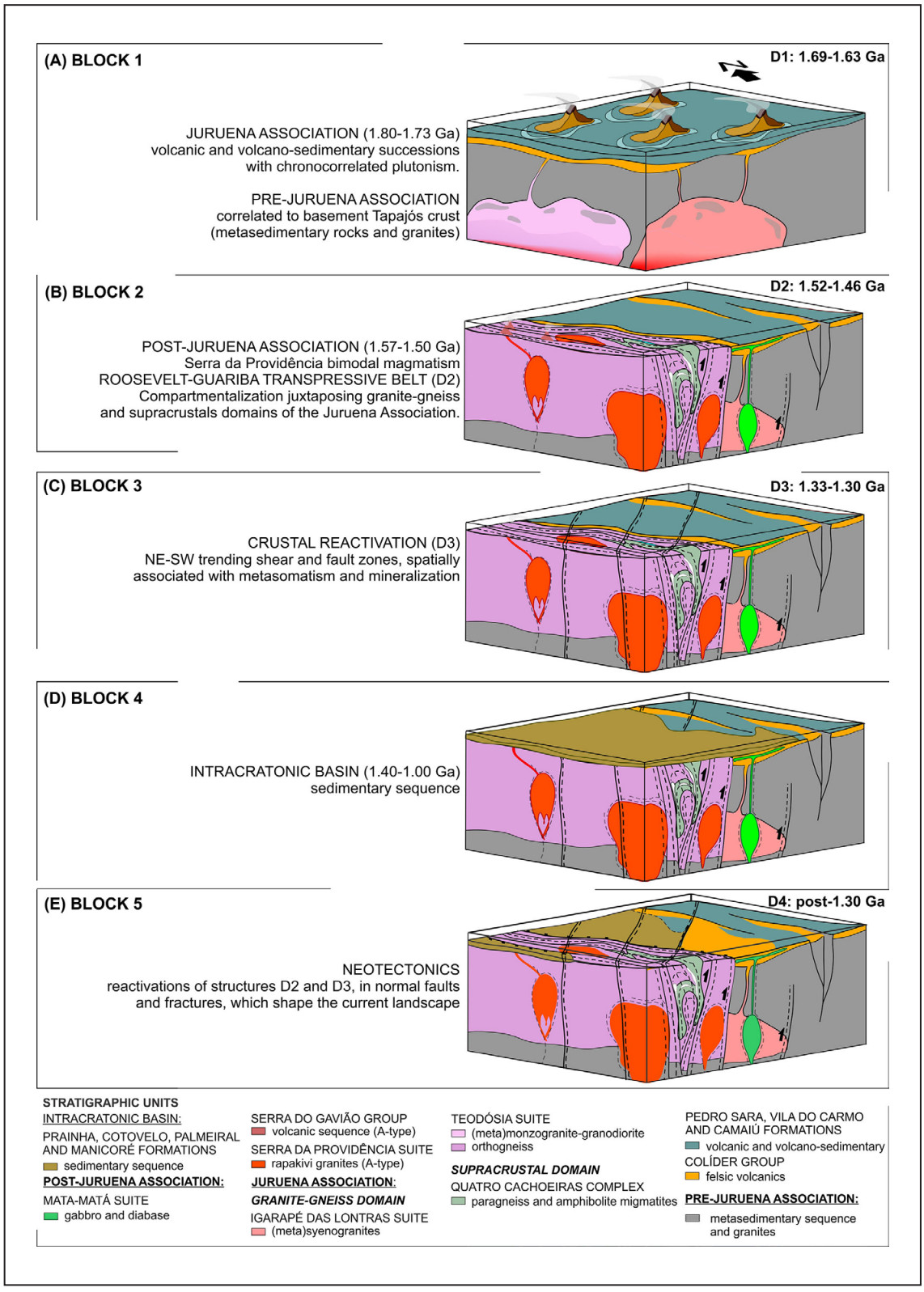

FIGURE 18. Schematic blocks show the structural history in the NNW of the Juruena Terrane, SE Amazonas State. They highlight the sequence of deformational events (A) D1; (B) D2; (C) D3; (D) intracratonic taphrogenesis; (E) D4.

to NW, along the RGTB. This configuration of event D1 (or DE1) (Almeida et al. 2016; Oliveira and Lira 2019; Reis and Ramos 2017; Reis et al. 2013; Simões et al. 2020) suggests a terrane formed in the context of a foreland basin whose basement is the Tapajós Crust. This basin covers the entire region, and its stratigraphic stacking pattern is preserved and free from deformation and metamorphism, throughout the Statherian, during the development of the Juruena Orogen (Figure 18A).

The RGTB was redefined in this study, reinforcing the existence of an important crustal-scale tectonic feature, predominantly with NW-SE direction. This feature controls the tectonic compartmentation of the NNW portion of the belt (southeast of Amazonas State, Figure 18B), which extends to the center-southeast portion (north of Mato Grosso), cross-cutting the entire Juruena Terrane and the EW regional structure (D1; 1.69-1.63 Ga, Scandolara et al. 2017) of the Juruena Complex (Ribeiro and Duarte 2011).

Internally, the RGTB presents subdomains singled out by the intensity of tectonic efforts, represented by high-temperature mylonites and schists in the northern section of the Roosevelt profile (moderate stress) and by migmatitic gneisses in the southern stretch of the Guariba profile (high stress). The granitoids and the deformed volcano sedimentary sequences present, respectively, high-temperature crystallographic features and metamorphic mineral assemblages, which characterize two metamorphic events: M1 in the upper amphibolite facies (>700°C) at medium pressure (3.3 to 6.0 kbar) and M2, retrometamorphism in the lower amphibolite facies (~550°C) at low pressure (1.0 to 3.0 kbar) (Lisboa 2019).

Based on these data, it can be concluded that the RGTB is an intracontinental lithospheric shear zone, generated by a tectono-thermal event of the Calymmian in the context of crustal reworking (1526-1466 Ma, Almeida ME, personal communication). The driving force for this intracontinental tectonic event is the propagation of stresses in pericratonic regions, caused by orogens such as Cachoeirinha (Ruiz et al. 2004), Rondoniano-San Ignacio (Bettencourt et al. 2010) and Içana (Almeida et al. 2013). This intracontinental crustal reworking process may have been triggered by thermal anomalies, attributed to the rise of the asthenospheric mantle in response to slab break-off in a post-orogenic tectonic context, which is compatible with the generation of a massive bimodal magmatism (Serra da Providência 1.57-1.51 Ga, Oliveira and Lira, 2019; Costa et al. 2016; Almeida et al. 2016; Scandolara et al. 2013) and the orogenic collapse marked by gravitational and transcurrent tectonics. Other important factors can also be considered; for example, the existence of thick and extensive cover of supracrustal successions and preexisting lithospheric weakness zones, associated with the formation of a foreland basin (Mcavaney et al. 2016; Piazolo et al. 2020; Raimondo et al. 2014; Silva et al. 2018).

Acknowledgments

The authors wish to express their gratitude to Dr. CA. Salazar (UFAM) and Dr. A. Ruiz (UFMT) for his helpful insights and suggestions. Many thanks to the valuable and unforgettable help from colleagues from CPRM on the several trips through the Amazonian lands, especially N. Reis, R. Bahia, U. Costa, L. Betiollo, A. Alves, AGH de Souza, M. Neves and F. Splendor (in memory). We would like to thank the Geological Service of Brazil (SGB/CPRM) for providing financial support for field analysis and surveys, and the Graduate Program in Geosciences (PPGGEO), from the Federal University of Amazonas (UFAM), for offering academic support during the development of the master's thesis that was the basis of this research. Finally, we are grateful to the JGSB's reviewers, who provided extremely constructive comments that helped enhance the quality of the original manuscript.

References

Albuquerque M.F.S., Horbe A.M.C., Botelho N.F. 2017. Genesis of manganese deposits in southwestern Amazonia: mineralogy, geochemistry and paleoenvironment. Ore Geology Reviews. 89, 270-289. https://doi.org/10.1016/j.oregeorev.2017.06.012

Almeida M.E., Macambira M.J.B., Santos J.O.S., Nascimento R.S.C., Paquette J.L. 2013. Evolução crustal do noroeste do Cráton Amazônico (Amazonas, Brasil) baseada em dados de campo, geoquímicos e geocronológicos. In: Simpósio de Geologia da Amazônia, 13., Belém. Available on line at: http://arquivos.sbg-no.org.br/BASES/SGA%2013.pdf / (accessed on 30 July 2021).

Almeida M.E., Oliveira A.C.S., Costa U.A.P. (org.). 2016. Geologia e recursos minerais da folha Sumaúma – SB.20-Z-D, estado do Amazonas, escala 1:250.000. Manaus, CPRM. Available on line at: https://rigeo.cprm.gov.br/handle/doc/18292 / (accessed on 15 July 2021).

Alves C. L., Sabóia A. M., Scandolara J. E., Ribeiro P. S. E., Martins E. G. 2013. Magmatismo Tipo A-2 Colíder-Pium no SE do Cráton Amazônico, Província Rondônia-Juruena - MT: litoquímica e geocronologia. In: Wankler F. L., Holanda E. C., Vasquez M. L. (ed.). Contribuições à geologia da Amazônia, 8. Belém, SBG Núcleo Norte, 26-44.

Araújo H.J.T., Rodarte J.B.M., Del'Arco J.O., Santos D.B., Barros A.M., Tassinari C.C.G., Lima M.I.C., Abreu A.S., Femandes C.A.C. 1978. Geologia. In: Projeto RADAMBRASIL. Folha SB. 20 Purus: geologia, geomorfologia, pedologia, vegetação e uso potencial da terra. Rio de Janeiro, DNPM, p. 19-128. Available on line at: https://biblioteca.ibge.gov.br/biblioteca-home?view=detalhes&id=224034 / (accessed on 15 July 2021).

Assis R.R. 2011. Depósitos auríferos associados ao magmatismo granítico do setor leste da Província de Alta Floresta (MT), Craton Amazônico = tipologia das mineralizações, modelos genéticos e implicações prospectivas. MSc Dissertation, Instituto de Geociências, Universidade Estadual de Campinas, Campinas, SP, 427 p. Available on line at: http://www.repositorio.unicamp.br/handle/REPOSIP/287710. / (accessed on 19 July 2021).

Betiollo L.M., Almeida M.E., Reis N.J., Bahia R.B.C., Splendor F., Costa U.A.P., Luzardo R. 2005. Magmatismo máfico calimiano (Sill Mata-Mata), rio Aripuana, Amazonas: implicações geológicas. In: Simpósio de Geologia da Amazônia, 11, 162–165. Available on line at: http://arquivos.sbg-no.org.br/BASES/Anais%2011%20Simp%20Geol%20Amaz%20Agosto-2005-Manaus.pdf / (accessed on 19 July 2021).

Bettencourt J.S., Leite W.B., Ruiz A.S., Matos R., Payolla B.L., Tosdal R.M. 2010. The Rondonian-San Ignacio Province in the SW Amazonian Craton: an overview. Journal of South American Earth Sciences, 29(1), 28-46. https://doi.org/10.1016/j.jsames.2009.08.006

Betts P., Armit R., Tiddy C., Armistead S., Ailleres L. 2019. Tectonic analysis of regional potential field data. ASEG Extended Abstracts, 2019, 1–5. https://doi.org/10.1080/22020586.2019.12073022

Betts P., Williams H., Stewart J., Ailleres L. 2007. Kinematic analysis of aeromagnetic data: looking at geophysical data in a structural context. Gondwana Research, 11(4), 582-583. https://doi.org/10.1016/j.gr.2006.11.007

Betts P.G., Valenta R.K., Finlay J. 2003. Evolution of the mount woods inlier, northern Gawler Craton, southern Australia: an integrated structural and aeromagnetic analysis. Tectonophysics, 366(1-2), 83-111. https://doi.org/10.1016/S0040-1951(03)00062-3

Brito R.S.C., Silveira F.V., Larizzatti, J. H. 2010. Metalogenia do distrito aurífero do rio Juma-Nova Aripuanã, AM. Informe de Recursos Minerais, Série Ouro, Informes Gerais, 17. Brasília, CPRM, 44 p. Available on line at: https://rigeo.cprm.gov.br/handle/doc/1753 / (accessed on 19 July 2021).

Bucher K., Grapes R. 2011. Petrogenesis of Metamorphic Rocks. 8th ed. Berlin, Heidelberg, Springer International Publishing. https://doi.org/10.1007/978-3-540-74169-5

Collins W.J. 2002. Hot orogens, tectonic switching, and creation of continental crust. Geology, 30(6), 535-538. https://doi.org/10.1130/0091-7613(2002)030<0535:HOTSAC>2.0.CO;2

Cordani U.G., Teixeira W. 2007. Proterozoic accretionary belts in the Amazonian. In: Hatcher Jr. R.D., Carlson M.P., McBride J.H., Catalán J.R.M. 4-D Framework of Continental Crust. Geological Society of America, 200, p. 297-320. https://doi.org/10.1130/2007.1200(14)

Cordani U.G., Teixeira W., D'Agrella-Filho M.S., Trindade R.I. 2009. The position of the Amazonian Craton in supercontinents. Gondwana Research, 15(3-4), 396-407. https://doi.org/10.1016/j.gr.2008.12.005

CPRM. 2010a. Projeto aerogeofísico Aripuanã: relatório final do levantamento e processamento dos dados magnetométricos e gamaespectométricos. Rio de Janeiro, Prospectors Aerolevantamentos e Sistemas. Programa Geologia do Brasil - PGB. Available on line at: https://rigeo.cprm.gov.br/handle/doc/10906 / (accessed on 19 July 2021).

CPRM. 2010b. Projeto aerogeofísico Sucunduri: relatório final do levantamento e processamento dos dados magnetométricos e gamaespectométricos. Rio de Janeiro, Prospectors Aerolevantamentos e Sistemas. Programa Geologia do Brasil - PGB. Available on line at: https://rigeo.cprm.gov.br/handle/doc/11047 / (accessed on 19 July 2021).

CPRM. 2015. Projeto aerogeofísico Branco-Machadinho: relatório final do levantamento e processamento dos dados magnetométricos e gamaespectrométricos, volume I – texto técnico. Rio de Janeiro, Lasa Prospecções. Programa Geologia do Brasil - PGB. Available on line at: https://rigeo.cprm.gov.br/handle/doc/21685 / (accessed on 19 July 2021).

Costa M.A.C., Sousa M.Z.A., Dall'Agnol R., Scandolara J.E., Ruiz A.S. 2016. Geochemistry and geochronology of the rapakivi granites and associated rocks in the midwest portion of the Serra da Providência composite batholith, SW of Amazonian craton, Rondônia, Brazil. Journal of South American Earth Sciences, 69, 194–212. https://doi.org/10.1016/j.jsames.2016.04.003

COSTA U.A.P., Oliveira A.C.S., Betiollo L.M., Splendor F., Bahia R.B.C., Almeida M.E., Reis N.J. 2013. Carta geológica: folha Sumaúma - SB.20-Z-D. Manaus, CPRM. Escala 1:250.000. Available on line at: https://rigeo.cprm.gov.br/handle/doc/18292 / Manter Oliveira et al 2014 / (accessed on 30 July 2021).

Cruz N.M. 1982. Palinoplancton de sedimentos paleozoicos do estado do Amazonas. Anais da Academia Brasileira de Ciências, 54(2), 355-363. Available on line at: http://memoria.bn.br/DocReader/DocReader.aspx?bib=158119&Pesq=sciencia&pagfis=26134 / (accessed on 19 July 2021).

Diener F.S., Polo H.J.O., Carneiro J.S.M. 2019. Geologia e recursos minerais da folha Rio Branco - SC.20-Z-B, estado do Mato Grosso. Goiânia, CPRM. Escala 1:250.000. Available on line at: https://rigeo.cprm.gov.br/handle/doc/21297 / (accessed on 19 July 2021).

Direen N.G., Cadd A.G., Lyons P., Teasdale J.P. 2005. Architecture of Proterozoic shear zones in the Christie Domain, western Gawler Craton, Australia: geophysical appraisal of a poorly exposed orogenic terrane. Precambrian Research, 142, 28–44. https://doi.org/10.1016/j.precamres.2005.09.007

Duarte T., Xavier R., Rodrigues J. 2019. A review of the geodynamic setting of the volcanic domain in the Juruena Magmatic Arc, southwestern Amazon Craton, Brazil, based on geochemical, U-Pb and Sm-Nd data. Journal of the Geological Survey of Brazil, 2(1), 37-73. https://doi.org/10.29396/jgsb.2019.v2.n1.4

Duarte T.B., Rodrigues J.B., Ribeiro P.S.E., Scandolara J.E. 2012. Tectonic evolution of the Juruena magmatic arc between the Aripuanã and Juruena rivers: northwest Mato Grosso state Brazil. Revista Brasileira Geociências, 42(4), 824-840. http://ppegeo.igc.usp.br/index.php/rbg/article/view/7973

Frasca A.A.S., Souza J.O., Lacerda Filho J.V., Oliveira C.C., Ribeiro P.S.E., Villas Boas P.F., Moreton L.C., Martins E.G., Borges F.R., Camargo M.A. 2002. Síntese da geologia do projeto PROMIN Alta Floresta, 1:500.000. In: Congresso Brasileiro de Geologia, 41, Sociedade Brasileira de Geologia, João Pessoa, p. 445. Available on line at: http://acervo.cprm.gov.br/rpi_cprm/docreaderNET/DocReader.aspx?bib=Anais&pesq=Congresso%20Brasileiro%20de%20Geologia / (accessed on 20 July 2021).

Goulart L.E.A., Silva A.R.C. 2019. Metalogenia das províncias minerais do Brasil: área Eldorado do Juma, estado do Amazonas. Informe de Recursos Minerais, Série Províncias Minerais do Brasil, 10. Manaus, CPRM 95 p. Available on line at: https://rigeo.cprm.gov.br/handle/doc/21325 / (accessed on 19 July 2021).

Hippertt J. 1999. Are S-C structures, duplexes and conjugate shear zones different manifestations of the same scale-invariant phenomenon? Journal of Structural Geology, 21(8-9), 975-984. https://doi.org/10.1016/S0191-8141(99)00047-4

Holdsworth R.E., Stewart M., Imber J., Strachan R.A. 2001. The structure and rheological evolution of reactivated continental fault zones: a review and case study. Geological Society, London, Special Publications, 184, 115-137. https://doi.org/10.1144/GSL.SP.2001.184.01.07

Jacobsen B.H. 1987. Case for Upward Continuation as a Standard Separation Filter for Potential-Field Maps. Geophysics 52, 1138-1148. https://doi.org/10.1190/1.1442378

Jessell M.W., Valenta R.K., Jung G., Cull J.P., Geiro A. 1993. Structural geophysics. Exploration Geophysics, 24(3-4), 599-602. https://doi.org/10.1071/EG993599

Lacerda Filho, J.V., Abreu Filho W., Valente C.R., Oliveira C.C., Albuquerque M.C. (org.). 2004. Geologia e recursos minerais do estado de Mato Grosso: texto explicativo. Cuiabá: CPRM, 2004. Available on line at: https://rigeo.cprm.gov.br/handle/doc/4871 / (accessed on 19 July 2021).

Leite J.A.D., Saes G. S., Macambira M.J.B. 2001. The Teles Pires volcanic province: a Paleoproterozoic silic-dominated large igneous province in southwest Amazon Craton and tectonic implications, in: Simpósio Sulamericano de Geologia Isotópica, 3, Sociedad Geologica de Chile, Pucón Chile, 180-183.

Leseane K., Betts P., Armit R., Ailleres L. 2020. Structural overprinting criteria determined from regional aeromagnetic data: an example from the Hill End Trough, East Gondwana. Tectonophysics, 797, 228660. https://doi.org/10.1016/j.tecto.2020.228660

Lisboa T.M. 2019. Metamorfismo de alta temperatura e média pressão de paragnaisses, anfibolitos e hornblenda-biotita gnaisse do Complexo Quatro Cachoeiras, Província Rondônia-Juruena, Rio Guariba - Amazonas. MSc Dissertation, Universidade Federal do Amazonas, Manaus, 117 p. Available on line at: https://tede.ufam.edu.br/handle/tede/7663 / (accessed on 30 July 2021).

Mcavaney S., Thiel S., Wade C. 2016. The Kalinjala shear zone: intracontinental shear zone or palaeosuture? In: Australian Earth Sciences Convention, Conference. Available on line at: https://www.researchgate.net/publication/308063554_The_Kalinjala_Shear_Zone_intracontinental_shear_zone_of_Palaeoproterozoic_palaeosuture / (accessed on 22 July 2021).

Meloni R.E., Simões M.S. 2019. As mineralizações de ouro do distrito aurífero Juma-SE do Amazonas. In: Simpósio Brasileiro de Metalogenia, 4, Gramado, p. 94-95. Available on line at: https://www.ufrgs.br/sbm/wp-content/uploads/2019/04/ANAIS.pdf / (accessed on 22 July 2021).

Meloni R.E., Simões M.S., Benevides P.R.R. 2018. Granitos de idade orosiriana no limite entre as províncias Tapajós-Parima e Rondônia-Juruena, região de Apuí – AM. In: Congresso Brasileiro de Geologia, 49, Rio de Janeiro, p. 938. Available on line at: http://cbg2018anais.siteoficial.ws/anexos/anais49cbg.pdf / (accessed on 22 July 2021).

Meloni R.E., Simões M.S., Benevides P.R.R., Lisboa T.M., Ramos M.N., Oliveira A.C. S., Silva A.R.C., Queiroz L.C. 2021. Mapa geológico: ARIM Sudeste do Amazonas. Manaus, SGB-CPRM. 1 mapa. Escala 1:500.000. Programa de Gestão Estratégica da Geologia, Mineração e Transformação Mineral: Ação Áreas de Relevante Interesse Mineral (ARIM). Available on line at: https://rigeo.cprm.gov.br/handle/doc/22194 / (accessed on 22 July 2021).

Montavão R.M.G., Bezerra P.E.L., Silva S.J., Araújo H.J.T., Prado P. 1984. Petrografia e química das rochas vulcânicas e piroclásticas do supergrupo Uatumã na parte sul da Amazônia. In: SYMPOSIUM AMAZONICO, 2, Manaus, p. 219-226.

Neder R.D., Figueiredo B.R., Beaudry C., Collins C., Leite J.A.D. 2000. The Expedito Massive Sulfide Deposit, Mato Grosso. Revista Brasileira de Geociências, 30, 222-225. https://doi.org/10.25249/0375-7536.2000302222225

Oliveira A.C.S. 2016. Evolução tectônica do Craton Amazonas na região Sudeste do estado do Amazonas: um estudo em múltiplas escalas com base na integração de dados geológico–estruturais e geofísicos. MSc Dissertation, Universidade Federal do Amazonas, Manaus, 81 p. Acesso: http://tede.ufam.edu.br/handle/tede/5158

Oliveira A.C.S., Oliveira A.A., Souza A.G.H., Costa U.A.P., Neves M.P., Benevides P.R.R., Lopes P.R.S., Lira R.R.C. 2014. Carta geologica: folha Rio Roosevelt - SC.20-X-B. Manaus, CPRM. Escala 1:250.000. Available on line at: https://rigeo.cprm.gov.br/handle/doc/21319 / (accessed on 30 July 2021).

Oliveira A.C.S., Costa U.A.P. 2011. Caracterização geológica – geofísica da ocorrência de ouro do garimpo gavião, região do apuí – sudeste do Amazonas: um depósito epitermal de baixa sulfetação? In: Simpósio de

Geologia da Amazônia, 12, Boa Vista, 48-51. Available on line at: http://arquivos.sbg-no.org.br/BASES/Anais%2012%20Simp%20Geol%20Boa%20Vista%20Outubro-2011.pdf / (accessed on 26 July 2021).

Oliveira A.C.S., Lira R.R.C. 2019. Geologia e recursos minerais da folha Rio Roosevelt – SC.20-X-B, estado do Amazonas. Manaus, CPRM. Escala 1:250.000. Available on line at: https://rigeo.cprm.gov.br/handle/doc/21319 / (accessed on 22 July 2021).

Oliveira A.C.S., Splendor F., Costa U.A.P., Betiollo L.M., Bahia R., Benedito C., Almeida M.E., Reis N.J. 2013. Carta geológica, folha Sumaúma SB.20-Z-D. Estado do Amazonas. Manaus, CPRM. Escala 1:250.000. 1 mapa. Available on line at: https://rigeo.cprm.gov.br/handle/doc/18292 / (accessed on 22 July 2021).

Oliveira R.G. 2008. Arcabouço geofísico, isostasia e causas do magmatismo cenozóico da província Borborema e de sua margem continental (nordeste do Brasil). PhD Thesis, Centro de Ciências Exatas e da Terra, Universidade Federal do Rio Grande do Norte, Natal, 2008, 415 p. Available on line at: https://rigeo.cprm.gov.br/handle/doc/270 / (accessed on 26 July 2021).

Passchier C.W., Trouw R.A.J. 2005. Microtectonics. 2nd ed. New York, Springer. DOI: 10.1007/3-540-29359-0

Payolla B., Bettencourt J.S., Tosdal R.M., Wooden J.L., Leite Jr. W.B., 2003a. Shrimp-Rg U-Pb zircon geochronology of high-grade paragneisses from ne Rondônia, SW Amazonian craton, Brazil: constraints on provenance and metamorphism. In: South American Symposium on Isotope Geology, 4, Salvador, p. 248–251. Available on line at: https://horizon.documentation.ird.fr/exl-doc/pleins_textes/divers17-05/010039206.pdf / (accessed on 30 July 2021).

Payolla B., Fetter A.H., Bettencourt J.S., Leite Jr. W.B., 2003b. U-Pb monazite ages from pelitic paragneisses in ne Rondônia, SW Amazonian craton: evidence for 1.54 Ga metamorphism. In: South American Symposium on Isotope Geology, 4, Salvador, p. 244–247. Available on line at: https://horizon.documentation.ird.fr/exl-doc/pleins_textes/divers17-05/010039206.pdf / (accessed on 30 July 2021).

Piazolo S., Daczko N.R., Silva D., Raimondo T. 2020. Melt-present shear zones enable intracontinental orogenesis. Geology, 48(7), 643–648. https://doi.org/10.1130/G47126.1

Pinho M.A.S.B., Chemale F., Van Schmus W.R., Pinho F.E.C. 2003. U-Pb and Sm-Nd evidence for 1.76-1.77 Ga magmatism in the Moriru region, Mato Grosso, Brazil: implications for province boundaries in the SW Amazon Craton. Precambrian Research, 126(1-2), 1-25. https://doi.org/10.1016/S0301-9268(03)00126-8

Quadros M.L.E.S., Palmeira L.C.M., Castro C.C. 2011. Geologia e recursos minerais da folha Rio Machadinho - SC.20-X-C, Estado de Rondônia, escala 1:250.000. Manaus, CPRM. Available on line at: https://rigeo.cprm.gov.br/handle/doc/11360 / (accessed on 26 July 2021).

Raimondo T., Hand M., Collins W.J. 2014. Compressional intracontinental orogens: Ancient and modern perspectives. Earth-Science Reviews, 130, 128-153. https://doi.org/10.1016/j.earscirev.2013.11.009

Reis N.J. 2006. Rochas carbonáticas da região de Apuí Amazonas. Informe de Recursos Minerais, Série Insumos Minerais para Agricultura, 12. Manaus, CPRM, 60 p. Available on line at: https://rigeo.cprm.gov.br/handle/doc/1739 / (accessed on 26 July 2021).

Reis N.J., Bahia R.B.C., Almeida M.E., Costa U.A.P., Betiollo L.M., Oliveira A.C.S., Splendor F. 2013. O supergrupo Sumaúma no contexto geológico da folha SB.20-Z- D (SUMAÚMA), sudeste do Amazonas: modo de ocorrência, discussão de idades em zircões detríticos e correlações no SW do Cráton do Amazonas. In: Wankler F.L., Holanda E.C., Vasques M.L. (ed.). Contribuições à geologia da Amazônia. Belém, Sociedade Brasileira de Geologia, v. 8, p. 199-222. Available on line at: http://arquivos.sbg-no.org.br/BASES/CGA%208.pdf / (accessed on 26 July 2021).

Reis N.J., Ramos M.N. 2017. Geologia e recursos minerais da folha Mutum – SB.20-Z-B, estado do Amazonas. Manaus, escala 1:250.000. Manaus, CPRM. Available on line at: https://rigeo.cprm.gov.br/handle/doc/17804 / (accessed on 26 July 2021).

Ribeiro P.S.E., Duarte T.B. 2010. Geologia e recursos minerais das folhas Rio Guariba SC.20-XD e Rio Aripuanã SC.21-V-C, escala 1:250.000. Goiânia, CPRM. Programa Geologia do Brasil (PGB). Levantamentos Geológicos Básicos. Available on line at: https://rigeo.cprm.gov.br/handle/doc/11355 / (accessed on 26 July 2021).

Rizzotto G.J., Alves C.L., Rios F.S., Barros A.S. 2019a. The western Amazonia igneous belt. Journal of South American Earth Sciences, 96, 102326. https://doi.org/10.1016/j.jsames.2019.102326

Rizzotto G.J., Alves C.L., Rios F.S., Barros M.A.S. 2019b. The Nova Monte Verde metamorphic core complex: tectonic implications for the southern Amazonian craton. Journal of South American Earth Sciences, 91, 154-172. https://doi.org/10.1016/j.jsames.2019.01.003

Rizzotto G.J., Quadros M.L.E.S. 2005. Geologia do Sudoeste do Craton Amazônico. In: Horbe A.M.C., Souza V.S. (ed.). Contribuições à geologia da Amazônia. Belém, Sociedade Brasileira de Geologia, v. 4, p. 69-84. Available on line at: http://arquivos.sbg-no.org.br/BASES/CGA%204.pdf / (accessed on 26 July 2021).

Ruiz A.S., Geraldes M.C., Matos J.B., Teixeira W., Van Schmus W.R., Schmitt R.S., 2004. The 1590-1520 Ma Cachoeirinha magmatic arc and its tectonic implications for the Mesoproterozoic SW Amazonian craton crustal evolution. Anais da Academia Brasileira de Ciências, 76, 807–824. https://doi.org/10.1590/s0001-37652004000400013

Santos J.O.S. 2003. Geotectônica dos escudos das Guianas e Brasil-Central. In: Bizzi L.A., Schobbenhaus C., Vidotti R.M., Gonçalves J.H. (ed.). Geologia, tectônica e recursos minerais do Brasil: texto, mapas e SIG. Brasília, CPRM, p. 169–226. Available on line at: https://rigeo.cprm.gov.br/handle/doc/5006 / (accessed on 26 July 2021).

Santos J.O.S., Rizzotto G.J., Potter P.E., McNaughton N.J., Matos R.S., Hartmann L.A., Chemale F., Quadros M.E.S. 2008. Age and autochthonous evolution of the Sunsás Orogen in West Amazon Craton based on mapping and U-Pb geochronology. Precambrian Res. 165(3-4), 120-152. https://doi.org/10.1016/j.precamres.2008.06.009

Santos S., Hartmann L.A., Gaudette H.E., Groves D.I., Mcnaughton N.J., Fletcher I.R., 2000. A new understanding of provinces of the Amazon craton based on integration of filed mapping and U-Pb geochronology. Gondwana Research, 3, 453-488. https://doi.org/10.1016/S1342-937X(05)70755-3

Scandolara J.E., Correa R.T., Fuck R.A., Souza V.S., Rodrigues J.B., Ribeiro P.S.E., Frasca A.A.S., Saboia A.M., Lacerda Filho J.V. 2017. Paleo-Mesoproterozoic arc-accretion along the southwestern margin of the Amazonian craton: the Juruena accretionary orogen and possible implications for Columbia supercontinent. Journal of South American Earth Sciences, 73, 223-247. https://doi.org/10.1016/j.jsames.2016.12.005

Scandolara J.E., Fuck R.A., Dall'Agnol R., Dantas E.L. 2013. Geochemistry and origin of the early Mesoproterozoic mangerite–charnockite–rapakivi granite association of the Serra da Providência suite and associated gabbros, central–eastern Rondônia, SW Amazonian Craton, Brazil. Journal of South American Earth Sciences, 45, 166-193. https://doi.org/10.1016/j.jsames.2013.03.003

Scandolara J.E., Ribeiro P.S.E., Frasca A.Ô.A.S., Fuck R.A., Rodrigues J.B. 2014. Geochemistry and geochronology of mafic rocks from the Vespor suite in the Juruena arc, Roosevelt-Juruena terrain, Brazil: implications for Proterozoic crustal growth and geodynamic setting of the SW Amazonian craton. Journal of South American Earth Sciences, 53, 20-49. https://doi.org/10.1016/j.jsames.2014.04.001

Scandolara J.E., Silva C.R., Rizzotto G.J., Quadros M.L.E.S., Bahia R.B.C. 1995. Compartimentação litoestrutural da porção ocidental do Cráton Amazônico – Estado de Rondônia. In: Simpósio Nacional de Estudos Tectônicos, 5, Gramado, 84–86.

Silva D., Piazolo S., Daczko N.R., Houseman G., Raimondo T., Evans L. 2018. Intracontinental orogeny enhanced by far-field extension and local weak crust. Tectonics, 37(12), 4421-4443. https://doi.org/10.1029/2018TC005106

Silva G.H., Leal J.W.L., Montavão R.M.G., Bezerra P.E.L., Pimenta O.N.S., Tassinari C.C.G., Fernandes C.A.C. 1980. Geologia. In: Projeto RADAMBRASIL. Folha SC. 21 Juruena: geologia, geomorfologia, pedologia, vegetação e uso potencial da terra. Rio de Janeiro, DNPM, pp. 21–116. Available on line at: https://biblioteca.ibge.gov.br/visualizacao/livros/liv24038.pdf / (accessed on 15 July 2021).

Silva G.H., Leal J.W.L., Salum O.A.L., Dall'Agnol R., Bassei M.A.S. 1974. Esboço geológico de parte da folha SC.21 Juruena. In: Congresso Brasileiro de Geologia, 28. Sociedade Brasileira de Geologia, Porto Alegre, v. 4, p. 309-320. Available on line at: http://www.sbgeo.org.br/home/pages/44 / (accessed on 26 July 2021).

Simões M.S., Meloni R.E., Santos J.O.S. 2020. Stratigraphy, depositional environments and zircon U-Pb (LA-ICP-MS) ages of the Statherian volcano-sedimentary Beneficente Group: Implications for tectonics and gold mineralization in SW of the Amazon Craton. Precambrian Research, 345, 105756. https://doi.org/10.1016/j.precamres.2020.105756

Simões M.S., Meloni R.E., Santos J.O.S. 2021. Idades de proveniência de zircões detríticos na Formação Igarapé Ipixuna: uma idade

máxima jurássica para o topo da Bacia do Alto Tapajós. In: Congresso Brasileiro de Geologia, 50, Brasília, p. 543. Available on line at: https://50cbg.com/wp-content/uploads/2021/07/50%C2%BACBG_Anais-Volume-2.pdf / (accessed on 15 July 2021).

Souza J.O., Frasca A.A.S., Oliveira C.C. (org.). 2005. Geologia e recursos minerais da folha Alta Floresta (relatório integrado): folhas Rio São João da Barra (SC.21- V-D), Alta Floresta (SC.21-X-C), Ilha 24 de Maio (SC.21-Z-A); Vila Guarita (SC.21- Z-B): estados de Mato Grosso e Pará. Escala 1:250.000. Brasília, CPRM. Programa Levantamentos Geológicos Básicos do Brasil - PLGB; Projeto Província Mineral de Alta Floresta (PROMIN-Alta Floresta). Available on line at: https://rigeo.cprm.gov.br/handle/doc/10246 / (accessed on 15 July 2021).

Spector A., Grant F.S. 1970. Statistical models for interpreting aeromacnetic data. Geophysics, 35(2), 293-302. https://doi.org/10.1190/1.1440092

Splendor F., Almeida M.E., Costa U.A.P., Bahia R.B.C. 2010. Geologia e petrografia da Suíte Serra da Providencia no sudeste do estado do Amazonas. In: Congresso Brasileiro de Geologia, 45, Belém. Available on line at: http://www.sbgeo.org.br/home/pages/44 / (accessed on 27 July 2021).

Stewart J.R., Betts P.G. 2010. Implications for proterozoic plate margin evolution from geophysical analysis and crustal-scale modeling within the western Gawler Craton, Australia. Tectonophysics, 483(1-2), 151–177. https://doi.org/10.1016/j.tecto.2009.11.016

Stewart J.R., Betts P.G., Collins A.S., Schaefer B.F. 2009. Multi-scale analysis of Proterozoic shear zones: an integrated structural and geophysical study. Journal of Structural Geology, 31(10), 1238-1254. https://doi.org/10.1016/j.jsg.2009.07.002

Tassinari C.C.G., Macambira M.J.B. 1999. Geochronological provinces of the Amazonian Craton. Episodes, 22(3), 174-182. https://doi.org/10.18814/epiiugs/1999/v22i3/004

Toczeck A., Schmitt R.S., Braga, M.A.S., Miranda F.P. 2019. Tectonic evolution of the Paleozoic Alto Tapajós intracratonic basin - A case study of a fossil rift in the Amazon Craton. Journal of South American Earth Sciences, 94, 102225. https://doi.org/10.1016/j.jsames.2019.102225

Trindade Netto G.B., Diener F.S., Fuentes D.B.V., REZENDE, E.S. (org). 2020. Áreas de relevante interesse mineral (ARIM): evolução crustal e metalogenia da região de Aripuanã. Informe de Recursos Minerais, Série Províncias Minerais do Brasil, 28. Goiânia, CPRM. Available on line at: https://rigeo.cprm.gov.br/handle/doc/21663/ (accessed on 22 July 2021).

Trouw R.A.J., Passchier C.W., Wiersma D.J. 2009. Atlas of mylonites- and related microstructures. Berlin, Springer Berlin Heidelberg. https://doi.org/10.1007/978-3-642-03608-8

Turcotte D.L. 1997. Fractals and chaos in geology and geophysics, Second Edition. Eos - Transactions American Geophysical Union, 79(29), 347. https://doi.org/10.1029/98EO00263

Winkler H.G.F. 1979. Petrogenesis of Metamorphic Rocks, 5th ed. New York,

Springer Science+Business Media, LLC. Available on line at: https://www.springer.com/gp/book/9781475742152 / (accessed on 19 July 2021).